Response of Amazonian forests to mid-Holocene drought: a model-data comparison

Received: 11 May 2021 | Revised: 22 September 2021 | Accepted: 25 September 2021

DOI: 10.1111/gcb.15929

Global Change Biology WILEY

PRIMARY RESEARCH ARTICLE

Response of Amazonian forests to mid-Holocene drought: A model-data comparison

Richard J. Smith[1] | Joy S. Singarayer[2] | Francis E. Mayle[1]

[1]Department of Geography and Environmental Science, School of Archaeology, Geography and Environmental Science (SAGES), University of Reading, Whiteknights, Reading, UK

[2]Department of Meteorology, University of Reading, Whiteknights, Reading, UK

Correspondence
Joy S. Singarayer, Department of Meteorology, University of Reading, Whiteknights, Reading, UK.
Email: j.s.singarayer@reading.ac.uk

Funding information
Natural Environment Research Council, Grant/Award Number: NE/L002566/1

Abstract

There is a major concern for the fate of Amazonia over the coming century in the face of anthropogenic climate change. A key area of uncertainty is the scale of rainforest dieback to be expected under a future, drier climate. In this study, we use the middle Holocene (ca. 6000 years before present) as an approximate analogue for a drier future, given that palaeoclimate data show much of Amazonia was significantly drier than present at this time. Here, we use an ensemble of climate and vegetation models to explore the sensitivity of Amazonian biomes to mid-Holocene climate change. For this, we employ three dynamic vegetation models (JULES, IBIS, and SDGVM) forced by the bias-corrected mid-Holocene climate simulations from seven models that participated in the Palaeoclimate Modelling Intercomparison Project 3 (PMIP3). These model outputs are compared with a multi-proxy palaeoecological dataset to gain a better understanding of where in Amazonia we have most confidence in the mid-Holocene vegetation simulations. A robust feature of all simulations and palaeodata is that the central Amazonian rainforest biome is unaffected by mid-Holocene drought. Greater divergence in mid-Holocene simulations exists in ecotonal eastern and southern Amazonia. Vegetation models driven with climate models that simulate a drier mid-Holocene (100–150 mm per year decrease) better capture the observed (palaeodata) tropical forest dieback in these areas. Based on the relationship between simulated rainfall decrease and vegetation change, we find indications that in southern Amazonia the rate of tropical forest dieback was ~125,000 km^2 per 100 mm rainfall decrease in the mid-Holocene. This provides a baseline sensitivity of tropical forests to drought for this region (without human-driven changes to greenhouse gases, fire, and deforestation). We highlight the need for more palaeoecological and palaeoclimate data across lowland Amazonia to constrain model responses.

KEYWORDS
Amazonia, biome resilience, climate change, dynamic global vegetation models, middle Holocene, palaeoecology

1 | INTRODUCTION

The fate of Amazonian forests is of great scientific concern, given their global importance in terms of the ecosystem services they provide. The tropical biomes of Amazonia host ~20%–25% of global terrestrial species (Dirzo & Raven, 2003; May et al., 2013). These biomes play an important role in the global carbon budget, constituting a large carbon reserve and a net sink for atmospheric CO_2 (Aragão et al., 2014; Pan et al., 2011; Phillips et al., 2009), and, through moisture recycling, influence regional and global climate patterns (Gash et al., 2004; Harper et al., 2014; Werth & Avissar, 2002). Although Amazonia contains one of the largest remaining areas of intact forest in the world (Potapov et al., 2017), decades of deforestation and forest fragmentation have left the ecosystems vulnerable (Malhi et al., 2008; Skole & Tucker, 1993; Soares-Filho et al., 2006). However, direct anthropogenic land use is not the only problem facing Amazonia over the coming century. As moisture availability is considered one of the most important limiting factors controlling Amazonia's forest productivity (Meir & Woodward, 2010), the potential for a drier future regional climate is particularly concerning (Malhi et al., 2008).

Simulations of future climate change vary between models, but overall suggest that Amazonia will be subject to a decrease in precipitation, with particular concern for a significant intensification of the dry season (e.g. Boisier et al., 2015; Duffy et al., 2015; Joetzjer et al., 2013). Detailed field-based ecological impact analyses have demonstrated the sensitivity of Amazonian forests to severe short-term drought events. For example, the Amazon Forest Inventory Network (RAINFOR; Malhi et al., 2002) project has provided evidence for increased tree mortality and substantial loss of biomass carbon in response to the 2005 and 2010 drought events (Doughty et al., 2015; Feldpausch et al., 2016; Phillips et al., 2009), raising concerns that Amazonian forests are finely balanced between being a carbon sink or source (Aragão et al., 2014; Brienen et al., 2015; Cavaleri et al., 2017; Gatti et al., 2014). However, the sensitivity of Amazonia to long-term climate change over the coming centuries is much more uncertain. Dynamic Global Vegetation Models (DGVMs) have become the primary way to investigate the large-scale, long-term responses of Amazonian vegetation to future climate change scenarios. However, projections from these DGVM studies vary considerably; outcomes include widespread replacement of rainforest with savannah (e.g. Betts et al., 2004; Cox et al., 2000; Huntingford et al., 2008), transition of humid to dry forests (e.g. Levine et al., 2016), and rainforest resilience (e.g. Cowling & Shin, 2006; Good et al., 2011, 2013; Huntingford et al., 2013). Reducing this uncertainty remains a key area of scientific focus.

The overall aim of this study is to use a palaeo-modelling approach to improve understanding of the uncertainties surrounding vegetation simulations of Amazonia and the scale of drought-induced forest dieback.

The premise of our approach, pioneered by the Palaeoclimate Modelling Intercomparison Project (Braconnot et al., 2011; Harrison et al., 2002; Joussaume & Taylor, 1995), is to run model simulations for a period in the past which had a climate state significantly different to that of the modern day, and for which there are sufficient palaeo-observational data to evaluate the model outputs. This methodology allows an assessment of model performance outside the range of modern forcings, providing potentially useful information about the credibility of future model projections (Braconnot et al., 2012; Harrison et al., 2015; Schmidt, 2010). The PMIP protocol also enables the community to focus on palaeo time slices that are in some ways roughly analogous to future projections and, in so doing, advance our understanding of Earth system sensitivities to those conditions (e.g. Haywood et al., 2019).

One of the key time periods that PMIP focuses on is the mid-Holocene, ca. 6000 years before present (6 ka BP), when levels of incoming solar radiation (insolation) differed from today due to changes in orbital forcing (Berger, 1978). Mid-Holocene atmospheric CO_2 levels were around 265 ppm, only slightly lower than those of the pre-industrial period (285 ppm). Palaeodata syntheses suggest that the mid-Holocene was potentially slightly warmer than present (possibly up to 0.7°C; Marcott et al., 2013). Southern-hemispheric tropical South America experienced a decrease in austral summer insolation levels at this time (Berger & Loutre, 1991), which restricted the seasonal southerly migration of the Inter-Tropical Convergence Zone (ITCZ; Haug et al., 2001; Singarayer et al., 2017). The decrease in austral summer insolation also reduced the strength of the South American summer monsoon (Baker & Fritz, 2015; Cruz et al., 2009), which is one of the major sources of precipitation for Amazonia (Raia & Cavalcanti, 2008; Silva & Kousky, 2012). Various palaeoclimate records show that much of Amazonia experienced a considerably drier mid-Holocene climate than present (Figure 1b), for example, significant lake-level reductions at Lake Titicaca on the Bolivian/Peruvian Altiplano (Baker et al., 2001), at Laguna La Gaiba in eastern lowland Bolivia (Whitney & Mayle, 2012; Whitney et al., 2011), and enriched stable oxygen isotope ($\delta^{18}O$) values from speleothems in southern Brazil (Bernal et al., 2016; Wang et al., 2007), the Peruvian Andes (Kanner et al., 2013) and the western Peruvian Amazon (van Breukelen et al., 2008; Cheng et al., 2013). There is also an indication of a mid-Holocene wet–dry dipole over Amazonia, with a recent speleothem record from Paraíso Cave (Wang et al., 2017) and several other records in the north-east suggesting wetter conditions (Figure 1b) while central, southern, and western Amazonia display drying.

There are a number of natural and anthropogenic drivers of vegetation change that may have significant impacts in the coming century. These drivers include increasing atmospheric CO_2, which may enhance plant growth through the fertilization effect and reduce transpiration due to increased stomatal resistance (Field et al., 1995; Langenbrunner et al., 2019), deforestation and forest degradation (Boers et al., 2017; Shukla et al., 1990), increases in forest fire frequency and severity (Nobre et al., 2016), as well as climate change itself and interactions between these factors. Here, we use the mid-Holocene as an approximate analogue for the drier climate conditions expected in future projections in order to explore the 'natural' sensitivity of Amazonian forests to drought. Although the mid-Holocene climate is by no means a perfect analogue for potential

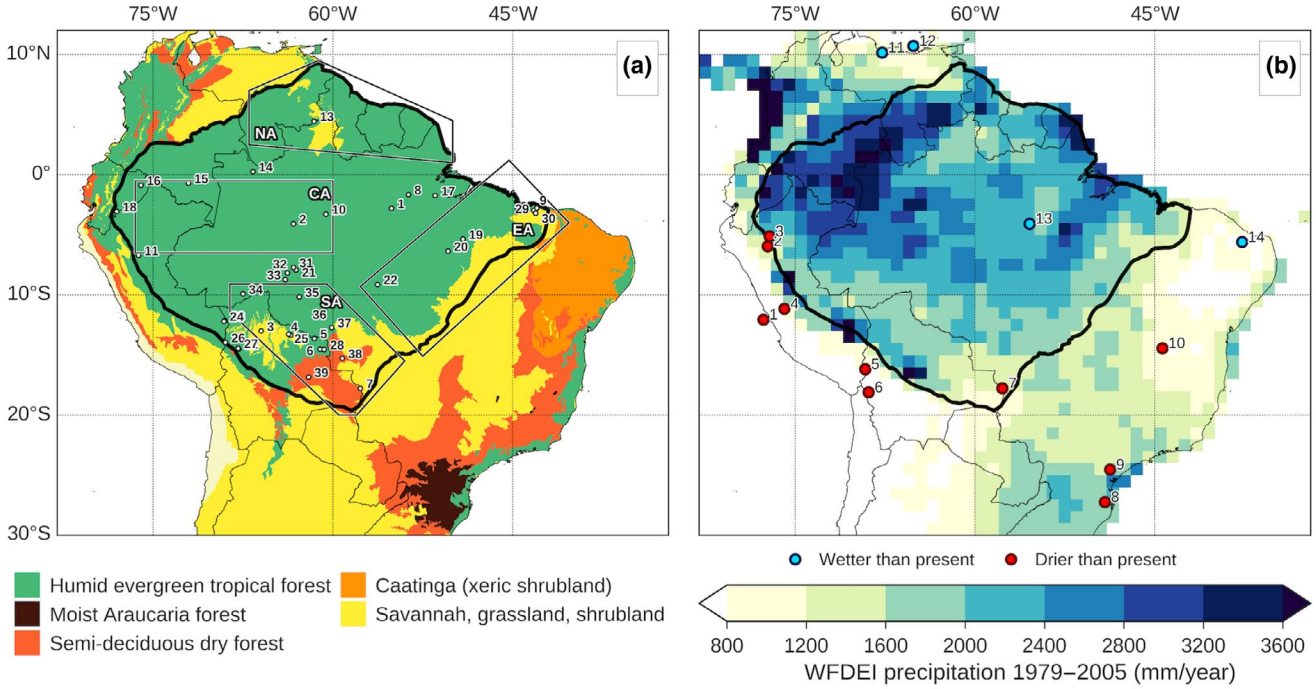

FIGURE 1 Overview maps of study area. (a) Map of potential broad-scale modern ecoregions modified from Olson et al. (2001), numbered points show locations of palaeoecological sites use in model-data comparison, see Table 2 for list. (b) Annual mean precipitation from the WFDEI dataset 1979–2005 (Weedon et al., 2014), numbered points show locations of key palaeoclimate sites that provide a qualitative estimate of relative dryness of the mid-Holocene (blue = MH wetter than present, red = MH drier than present), see Table 3 for list. The solid black outline in (a) and (b) marks the delineation of our definition of 'Amazonia'. Polygons in (a) outline key areas referenced throughout this study: Northern Amazonia (NA), Central Amazonia (CA), Eastern Amazonia (EA), Southern Amazonia (SA)

future climate change (most notably with respect to atmospheric CO_2 levels and temperature), it does provide a means for examining how the models predict vegetation response to large-scale, long-term, precipitation changes in Amazonia, thus providing insights into those regions one can expect to be most vulnerable to a prolonged drier climate in the future.

Previous studies have shown that two important sources of uncertainty in vegetation model simulations derive from (1) which DGVM is used (e.g. Galbraith et al., 2010; Sitch et al., 2008) and (2) the climate data used to drive the DGVM (e.g. Good et al., 2013; Schaphoff et al., 2006; Zhang et al., 2015). Therefore, to incorporate these sources of uncertainty into our analysis, our ensemble consists of simulations using three different DGVMs driven with the mid-Holocene climate simulations from seven of the climate models that participated in PMIP phase 3 (PMIP3; Braconnot et al., 2011). The simulations are compared with a multiproxy palaeovegetation dataset compiled in Smith and Mayle (2018). This allows us to assess the relative skill of each model combination and help determine those regions of Amazonia for which we have the most/least confidence in the mid-Holocene vegetation simulations.

The specific aims of our study are to resolve two key questions:

1. Which of the climate-vegetation model combinations perform better in a model-data comparison of mid-Holocene Amazonian biomes?
2. What do the models reveal about the geographical scale of tropical forest dieback due to drier mid-Holocene conditions?

2 | MATERIALS AND METHODS

2.1 | Geographical setting

The area we define as 'Amazonia' in this study is shown in Figure 1. This is predominantly based on the broad *sensu latu* definition of Amazonia, which contains most of the lowland humid evergreen forest biome, including the 'Guyanas' of northern South America (Eva & Huber, 2005). We extend the eastern edge of the defined area into the Cerrado savannah/evergreen forest ecotone and extend the southern edge to incorporate the Chiquitano dry forest of eastern Bolivia (Figure 1a), as we are interested in potential ecotonal shifts in these bordering regions.

2.2 | Dynamic global vegetation models (DGVMs)

Three DGVMs were used in this study: the Joint UK Land Environment Simulator (JULES) version 4.9 (Best et al., 2011; Clark et al., 2011), the University of Sheffield Dynamic Global Vegetation Model (SDGVM) (Woodward & Lomas, 2004; Woodward et al.,

TABLE 1 PMIP3 climate models used in this study

Model name	Modelling centre	Original atmospheric grid resolution	Dynamic vegetation	Reference(s)
CNRM-CM5	Centre National de Recherches Météorologiques/Centre Europeen de Recherche et Formation Avancees en Calcul Scientifique (CNRM-CERFACS)	T127 (~1.4° × 1.4°) L31	No	Voldoire et al. (2013)
CSIRO-Mk3-6-0	Commonwealth Scientific and Industrial Research Organisation/Queensland Climate Change Centre of Excellence (CSIRO-QCCCE)	T63 (~1.875° × 1.875°) L18	No	Gordon et al. (2002; 2010), Jeffrey et al. (2013)
FGOALS-s2	Laboratory of Atmospheric Sciences and Geophysical Fluid Dynamics/Institute of Atmospheric Physics, Chinese Academy of Sciences (LASG-IAP)	R42 (~1.66° × 2.81°) L26	Yes	Bao et al. (2013)
GISS-E2-R	National Aeronautics and Space Administration (NASA) Goddard Institute for Space Studies (GISS)	2° × 2.5° L40	No	Schmidt, Kelley, et al. (2014)
HadGEM2-CC	Met Office Hadley Centre (MOHC)	1.875° × 1.25° L38	Yes	Collins et al. (2011), Martin et al. (2011)
IPSL-CM5A-LR	Institut Pierre Simon Laplace (IPSL)	1.875° × 3.75° L39	Yes	Kageyama, Braconnot, Bopp, Caubel, et al. (2013); Kageyama, Braconnot, Bopp, Mariotti, et al. (2013); Marti et al. (2010)
MIROC-ESM	Model for Interdisciplinary Research on Climate, University of Tokyo (MIROC)	T42 (~2.8125° × 2.8125°) L80	Yes	Sueyoshi et al. (2013), Watanabe et al. (2011)

1995), and the Integrated Biosphere Simulator (IBIS) version 2.6b4 (Foley et al., 1996; Kucharik et al., 2000). This study focuses predominantly on the simulation of vegetation dynamics within these models, although they have been developed to include water and energy exchange between vegetation, soil, and atmosphere. All three of these vegetation models split each grid cell into fractions of different plant functional types (PFTs; see Table S1.1), simulating vegetation dynamics and competition between these PFTs using a 'big-leaf' approach. More detailed information about each DGVM can be found in the original model description papers. Details of the soil input data for each DGVM are shown in Appendix S3.

2.3 | Experimental design

For each DGVM, a control 'pre-industrial' simulation was conducted using historical climate data and pre-industrial levels of CO_2 of 285 ppm, as defined in the PMIP3 pre-industrial experiment (Meinshausen et al., 2011; Taylor et al., 2012). Land-use change was omitted for the control runs, so can be thought of as *potential* modern vegetation simulations. The mid-Holocene simulations were forced with climate data from the PMIP3 climate model simulations and CO_2 concentration of 280 ppm, as defined in the PMIP3 mid-Holocene experiment (Braconnot et al., 2011). An initial spin-up phase was conducted in all vegetation simulations to allow carbon and vegetation fields to equilibrate before the transient runs. Each DGVM required a slightly different spin-up procedure. JULES is the most computationally expensive model to run, so an accelerated spin-up procedure was used that ran for ~400 years rather than the >1000 years using a 'standard' procedure (Harper et al., 2014). For IBIS, a modified spin-up procedure was used, increasing the spin-up length from the default 150 years to 400 years. As SDGVM is the most computationally inexpensive model to run, a long spin-up of 1500 years was used.

2.4 | Climate data

For the control pre-industrial simulation, the climate data come predominantly from the WATCH Forcing Data ERA-Interim (WFDEI) dataset, which contains climate data in 3-hourly time steps created specifically for use in hydrological and land surface models (Weedon et al., 2014). WFDEI has data for most of the required climate variables except for cloud cover (for which we use data from the Climatic Research Unit [CRU] TS v4.01 dataset (Harris & Jones, 2017; Harris et al., 2014)), and relative humidity (for which we used a conversion equation using specific humidity, temperature, and surface pressure—see Appendix S2 for full details). All the climate data were re-gridded to a spatial resolution of 1.0° × 1.0° for the period 1979–2005. The modern WFDEI climate data were combined with pre-industrial atmospheric CO_2 levels (as outlined in the previous section) to drive the DGVMs in the control pre-industrial simulation. This assumes that the climate for the pre-industrial was similar to

present, and importantly enables us to force the DGVMs with realistic spatial climate patterns and seasonality.

The climate fields used for the mid-Holocene runs were processed from prior simulations of seven of the CMIP5 GCMs that ran the mid-Holocene PMIP3 experiment (Table 1). These climate models span a range of potential climates for the mid-Holocene, allowing us to explore the response of vegetation to different mid-Holocene climate scenarios. As the climate models exhibit considerable biases for Amazonia (Malhi et al., 2009), we applied an anomaly approach to produce more realistic (spatially and temporally) climate fields for the mid-Holocene. For each climate variable (except wet days, temperature delta, and temperature range), after re-gridding to the 1.0° × 1.0° spatial resolution, monthly anomalies were calculated between the mid-Holocene and pre-industrial PMIP3 experiments. These monthly anomalies were then added to the WFDEI 3-hourly climate data to create a 3-hourly mid-Holocene dataset. The variables of wet days, temperature delta, and temperature range were then calculated from the resultant precipitation and temperature fields. The three DGVMs each require slightly different driving climate fields (Table S2.1). IBIS and SDGVM required monthly averages to be calculated from the 3-hourly mid-Holocene data.

2.5 | Palaeo-data reconstructions

The mid-Holocene represents a time period for which there are a growing number of palaeoenvironmental data records for tropical South America (e.g. see Marchant et al., 2009; Prado et al., 2013; Smith & Mayle, 2018). The palaeoecological vegetation reconstructions used in this study are the Amazonian subset of the more geographically extensive multi-proxy data synthesis of tropical South America from Smith and Mayle (2018), see Table 2. These vegetation reconstructions are based primarily on fossil pollen assemblages, with complementary information derived from stable carbon isotopes, phytoliths, and charcoal analyses. This dataset qualitatively assigns a vegetation classification to each palaeoecological record based on a critical evaluation of the original authors' interpretations of their proxy data. In some cases, a combination of two classifications was assigned, when it was deemed that the vegetation cover was a mixture of vegetation types. Additionally, this dataset considers the spatial scale of vegetation cover recorded at each site. For example, in palynology, it is widely accepted that basin area is roughly proportional to the spatial scale that the pollen assemblage from that basin represents, for example, large (small) lakes collect pollen from regional (local) source areas (Davis, 2000; Sugita, 1994, 2007; Sugita et al., 1999). This is important to consider, as the relatively coarse-grid resolution of the model output (1.0° × 1.0°) will clearly be more comparable with reconstructions from larger basins. However, we do not dismiss the smaller-scale reconstructions as (1) the already small number of sites across Amazonia would be reduced even further; (2) clusters of smaller sites can help us infer the degree of fine-grain heterogeneity/homogeneity in vegetation cover that cannot be captured by coarse grain, regional reconstructions from larger basins; and (3) changes occurring at smaller sites may still reflect regional-scale climate change (e.g. Carson et al., 2014; Smith et al., 2021). The palaeoclimate records shown in Figure 1b were chosen for their ability to give qualitative estimates of the relative changes in precipitation between the mid-Holocene and present, which, like the palaeoecological records, were based on the original authors' interpretation of the data. These records provide direct evidence of mid-Holocene precipitation changes, for example through the changes of stable oxygen isotope ($\delta^{18}O$) values in speleothems or lake-level reconstructions (see Table 3 for full list).

2.6 | Classification method

The palaeo-data that we use for comparison with the mid-Holocene model outputs are given as qualitative classifications (see Smith and Mayle (2018) for justification), whereas the model outputs are continuous quantitative data. Therefore, qualitative classification of the model output is necessary to facilitate direct comparisons between the simulations and observations. A simple approach would be to use the most dominant PFT (in terms of percentage cover) in a grid cell as the classification, but this may not be suitable in this study for several reasons, including (1) the DGVMs differ in their representation of PFT coverage making inter-model comparisons difficult, for example JULES typically simulates a mixture of PFTs, whereas IBIS generally simulates a single PFT that dominates a grid cell (e.g. see Figure 2c); (2) in some cases, the dominant PFT may be only marginally dominant over other PFTs and may not reflect the actual overall biome, especially in ecotonal areas where a mixture of vegetation types may occur; (3) all the DGVMs perform poorly in differentiating between tree cover and grass cover in savannah ecosystems such as the Cerrado biome (Figure 2), a difficult area to model as important, yet relatively poorly understood, controls on tree density here include edaphic factors and fire frequency (Baudena et al., 2015; Langan et al., 2017; Murphy & Bowman, 2012). Fire processes are often not included or under-estimated in DGVMs. Instead, we use a statistical approach to classification, allowing us to utilize a variety of model output variables that, in combination, may provide a more accurate estimation of the overall biome of a given grid cell.

A linear discriminant analysis (LDA) approach was chosen, as it is a popular method in machine-learning classification problems and has been successfully used for modern ecological classification using physical attributes of vegetation (e.g. Cutler et al., 2007; Zizka et al., 2014), including over South America (Gond et al., 2011). LDA was found to be more accurate than several other classification techniques (random forest method, multi-class logistic regression model, multi-class multinomial logistic regression model, quadratic discriminant analysis) when trained on a random 70% of the full dataset for this study.

LDA is a supervised dimensionality reduction technique which searches for the linear combination of features (i.e. model output variables) that best discriminate between multiple classes (i.e. vegetation classification). In practice, this means that, for each DGVM, an

TABLE 2 List of palaeoecological sites. ID refers to location number in Figure 1a

ID	Site name	Size	Lon. (°E)	Lat. (°N)	Reference(s)
1	Lago Tapajós	L	−55.1	−2.79	Irion et al. (2006)
2	Coari Lake	L	−63.3	−4.06	Horbe et al. (2011)
3	Lago Rogaguado	L	−65.99	−13.0	Brugger et al. (2016)
4	Laguna Orícore	L	−63.53	−13.35	Carson et al. (2014)
5	Laguna Bella Vista	L	−61.55	−13.62	Burbridge et al. (2004), Mayle et al. (2000)
6	Laguna Chaplin	L	−61.08	−14.5	Burbridge et al. (2004), Mayle et al. (2000)
7	Laguna La Gaiba	L	−57.72	−17.76	Whitney et al. (2011)
8	Prainha lake cluster: Lake Santa Maria/Lake Geral/Lake Saracuri/Lake Comprida	M	−53.7	−1.64	Bush et al. (2000), Bush, Silman, and De Toledo (2007)
9	Lagoa do Caçó	M	−43.25	−2.96	Ledru et al. (2006), Pessenda et al. (2004, 2005), Sifeddine et al. (2003)
10	Lago Calado	M	−60.58	−3.27	Behling et al. (2001)
11	Lake Sauce	M	−76.22	−6.71	Bush et al. (2016)
12	Lake Santa Rosa	M	−67.87	−14.48	Urrego et al. (2013)
13	El Paují	S	−61.58	4.47	Montoya, Rull, and Nogué (2011)
14	Lake Pata	S	−66.68	0.27	Bush, De Oliveira, et al. (2004), Colinvaux et al. (1996)
15	Pantano de Monica	S	−72.07	−0.7	Behling et al. (1999)
16	Maxus 4	S	−76.03	−0.87	Weng et al. (2002)
17	Rio Curuá	S	−51.46	−1.74	Behling and da Costa (2000)
18	Lake Ayauchi	S	−78.03	−3.05	Liu and Colinvaux (1988), McMichael et al. (2012)
19	Lake Marabá	S	−49.15	−5.35	Guimarães et al. (2013)
20	Carajás/Pántano da Maurítia/Lagoa da Cachoeira	S	−50.39	−6.36	Absy et al. (1991), Sifeddine et al. (1994, 2001)/Hermanowski, Costa, and Behling (2012), Hermanowski, da Costa, Carvalho, et al. (2012)/Hermanowski et al. (2014)
21	Humaitá HU01	S	−63.08	−7.92	Cohen et al. (2014)
22	Lago do Saci	S	−56.27	−9.12	Fontes et al. (2017)
23	Lake Parker	S	−69.02	−12.14	Bush, Silman, and De Toledo (2007), Bush, Silman, and Listopad (2007)
24	Lake Gentry	S	−69.1	−12.18	Bush, Silman, and De Toledo (2007), Bush, Silman, and Listopad (2007)
25	Laguna Granja	S	−63.71	−13.26	Carson et al. (2014)
26	Lago Consuelo	S	−68.98	−13.95	Bush et al. (2004)
27	Lake Chalalán	S	−67.92	−14.43	Urrego et al. (2013)
28	Huanchaca	S	−60.73	−14.54	Maezumi et al. (2015)
29	Barreirinhas soil profile collection 1	XS	−43	−2.75	Pessenda et al. (2004)
30	Barreirinhas soil profile collection 2	XS	−43.09	−3.2	Pessenda et al. (2004)
31	Humaita soil profiles collection 1	XS	−63.3	−7.7	de Freitas et al. (2001), Pessenda et al. (2001)
32	Humaita soil profiles collection 2	XS	−63.8	−8.17	de Freitas et al. (2001), Pessenda et al. (2001)
33	Humaita soil profiles collection 3	XS	−63.97	−8.72	de Freitas et al. (2001)
34	Jaco Sá soil profiles	XS	−67.52	−9.92	Watling et al. (2017)
35	Ariquemes	XS	−62.82	−10.17	Pessenda et al. (1998)
36	Pimenta Bueno	XS	−61.2	−11.79	Pessenda et al. (1998)

TABLE 2 (Continued)

ID	Site name	Size	Lon. (°E)	Lat. (°N)	Reference(s)
37	Vilhena	XS	−60.12	−12.7	Pessenda et al. (1998)
38	Pontes e Lacerda	XS	−59.23	−15.27	Gouveia et al. (2002)
39	Laguna Sucuara	XS	−62.04	−16.83	Zech et al. (2009)

Note: Size refers to basin size, an indication of the spatial scale each site's vegetation reconstruction represents: L = Large, M = Medium, S = Small, XS = Extra-small, see Smith and Mayle (2018) for more information.

LDA algorithm is trained using a set of the output variables from the modern control simulations and the vegetation classifications based on those shown in Figure 1a. This allows the algorithm to 'learn' what combination of the simulated output variables would be expected for each vegetation class. Then, for a given DGVM, the LDA can be fed with the mid-Holocene simulated output variables for each grid cell, which allows the algorithm to predict which vegetation class the grid cell most likely belongs to. For this study, the model output variables used in each LDA include the following: the fraction of three PFTs (evergreen broadleaf, deciduous broadleaf, and C4 grass), vegetation biomass, soil carbon, soil moisture content, leaf area index (LAI), and net primary productivity (NPP). To simplify the classification problem, we only considered three vegetation classes: humid evergreen tropical forests (HETF), semi-deciduous tropical dry forest (SDTF), and savannah (SAV).

3 | RESULTS

3.1 | Modern vegetation simulations

The results of each DGVM PI control simulation, driven with modern observational climate data, are shown in Figure 2 as PFT percentage covers of evergreen broadleaf, deciduous broadleaf, and C4 grass. We compare these with the modern potential ecoregions (Figure 2a,e,i) rather than satellite observational data as much of the Brazilian Cerrado, eastern Amazonia, and the dry forest regions have undergone extensive anthropogenic land use in the last few decades (Malhi et al., 2008; Soares-Filho et al., 2006), which was not included in these simulations. Here it is important to note that the modern potential ecoregions have well-defined edges to their extent that will not be present in the modelled PFTs as PFTs are distinctly different from ecoregions and several PFTs can coexist within each grid cell. However, the comparison gives an indication of how well the DGVMs simulate present-day Amazonia.

All DGVMs reproduce the core of the Amazonian humid evergreen forest reasonably well. Both JULES and SDGVM show denser evergreen broadleaf cover in the central and western parts than other parts of Amazonia (Figure 2b,d), whereas IBIS shows less spatial variation, essentially simulating 100% evergreen broadleaf cover across the entire region (Figure 2c). In southern Amazonia, JULES captures the southern Amazonian ecotone in north-east Bolivia reasonably well, including peaks in deciduous broadleaf where the Chiquitano dry forest (eastern Bolivia) is located (Figure 2e,f). SDGVM also shows a slight decrease in evergreen broadleaf (and corresponding increase in deciduous broadleaf) in this region, though not as pronounced as with JULES (Figure 2d,h). Conversely, IBIS simulates extensive evergreen broadleaf in north-east Bolivia, with no indication of a mix with semi-deciduous forest (Figure 2c). In eastern Amazonia, IBIS reproduces the location of the eastern ecotone of the Amazonian humid evergreen tropical forests reasonably well (Figure 2c), although the model simulates a transition to deciduous broadleaf rather than the expected C4 grass of the cerrado savannah biome. Similar results are seen in SDGVM, though the ecotone boundary is slightly further east than in IBIS (Figure 2d). JULES simulates evergreen broadleaf well into the cerrado savannah (Figure 2b). In general, all models have difficulty reproducing the C4 grass dominated landscape of the cerrado savannah, probably due to the complex mix of edaphic and fire-related processes that influence vegetation cover here and which, in the case of fire, were not represented in the DGVMs (Baudena et al., 2015; Castanho et al., 2013; Marthews et al., 2014).

3.2 | Mid-Holocene climate anomalies

Overall, the DGVMs simulate the extent of Amazonian evergreen broadleaf reasonably well when forced with the same observational modern climate data. To assess their efficacy at simulating mid-Holocene vegetation, we first examine inter-model variation in simulated mid-Holocene climate. Figure 3 shows the annual precipitation anomalies between the mid-Holocene and pre-industrial for each climate model. Except for CSIRO-Mk3-6–0 (Figure 3h), all models simulate an overall negative anomaly averaged for the whole of Amazonia. For comparison, the surface air temperature anomalies are shown in Figure S4.2. The annual average mid-Holocene changes are mostly $< \pm 0.7$°C. Models that have larger drying anomalies in precipitation tend to have more areas with positive temperature anomalies and vice versa. MIROC-ESM has larger temperature anomalies relative to the other models but similar or smaller percentage precipitation changes (Figure 3; Figure S4.3).

Although the overall mid-Holocene precipitation change is negative in most models, the spatial distribution of the direction and magnitude of changes varies quite considerably between the models. GISS-E2-R, HadGEM2-CC, and FGOALS-s2 all simulate a drier mid-Holocene across most of Amazonia. However,

GISS-E2-R has much stronger drying in the north (Figure 3b); HadGEM2-CC has small areas of increased mid-Holocene precipitation in central Amazonia, but with negative anomalies to the north and south (Figure 3c); FGOALS-s2 has fairly consistent but weak drying across the whole region (Figure 3d). CNRM-CM5 simulates most drying in the east and south, with little change in the west of Amazonia (Figure 3e). MIROC-ESM has weak negative anomalies across much of Amazonia, but with increases in mid-Holocene precipitation along the northeast coastline (Figure 3f). IPSL-CM5A-LR (Figure 3g) has a north-to-south split in the anomalies, with a wetter north and a drier south; however, these anomalies are relatively small. Finally, CSIRO-Mk3-6-0 is the model with the most widespread positive anomalies, particularly in the north and east (Figure 3h). The models with the larger negative anomalies in the mid-Holocene are also the models that have a wetter pre-industrial (Figure S4.1) and compare better with the present-day observations (Figure 3a).

To explore the changes to the seasonality of simulated mid-Holocene precipitation, Figure 4 presents the annual precipitation cycle anomalies of each climate model for four key areas of Amazonia. In northern Amazonia (Figure 4a), most of the climate models simulate a precipitation decrease during the late wet season and into the early dry season (July–October), but a slight increase during the late dry season and into the early wet season (January–April). The exceptions are GISS-E2-R and CSIRO-Mk3-6-0, which simulate decreases/increases throughout the year, respectively. In central Amazonia (Figure 4b), most climate models simulate precipitation decreases during the wet season (February–May) and increases during the dry season (July–September), thus slightly reducing the seasonality of precipitation in this area. CNRM-CM5 is an exception, showing the opposite trend (wetter wet season, drier dry season). In eastern Amazonia (Figure 4c), most climate models simulate precipitation decreases through the wet season (December–March), with the exception of CSIRO-Mk3-6-0). Changes are negligible during the early dry season, then during the late dry season (August–October) there is a general agreement of a decrease in precipitation. Finally, southern Amazonia (Figure 4d) shows similar patterns to eastern Amazonia, with all climate models simulating a drier wet season (December–March) and only small changes during the early dry season. However, there is disagreement among models during the late dry season with a roughly 50/50 split in models simulating an increase/decrease in precipitation from August to October.

Unfortunately, there is a lack of independent palaeoclimate data across the Amazonian lowlands, with the majority of speleothem and lake-level records coming from the Andean mountain range or southern/eastern Brazil (Figure 1b), outside our defined study region. Additionally, it is difficult to make quantitative estimates of precipitation changes from the available palaeoclimate records. These factors make it difficult to fully benchmark the simulated mid-Holocene precipitation across Amazonia from the different climate models. Nevertheless, some important qualitative comparisons can be made and will be discussed in the relevant sections of the discussion section below.

3.3 | Simulated mid-Holocene PFT anomalies

For each area of Amazonia, the average mid-Holocene versus control anomalies for the evergreen broadleaf, deciduous broadleaf, and C4 grass PFTs are shown in Figure 5, in relation to the anomalies in annual precipitation. In the areas of northern, eastern, and southern Amazonia, similar overall trends are shown with respect to the PFTs' changes versus precipitation change. Generally, evergreen broadleaf anomalies exhibit a positive correlation with precipitation anomalies (i.e. precipitation decrease associated with evergreen broadleaf decrease), as expected, whereas both deciduous broadleaf and C4 anomalies exhibit a negative correlation with precipitation anomalies (i.e. precipitation decrease associated with increase in deciduous broadleaf/C4). In central Amazonia, there is very little change in any of the PFTs to any amount of precipitation change in all three DGVMs (Figure 5d-f).

Despite the overall trends being similar, the sensitivities of the DGVMs' PFTs to precipitation change vary considerably. For example, SDGVM is much less sensitive to precipitation decrease than IBIS and JULES, particularly in northern Amazonia. In eastern Amazonia, IBIS simulates much larger changes than SDGVM and JULES, predominantly due to IBIS not simulating the coexistence of the evergreen broadleaf and deciduous broadleaf PFTs very well (Figure 2c,g); for example, if a grid cell simulates decreases in evergreen broadleaf, it will be a ~100% PFT shift, thus skewing the overall regional mean. Further detailed descriptions are shown found in Appendix S5.

3.4 | LDA Classification maps and model-data comparison with palaeoecological reconstructions

Figure 6 presents the result of the mid-Holocene LDA biome classifications for each model combination, allowing us to directly compare the mid-Holocene vegetation simulations with the palaeoecological observations for Amazonia. Perhaps unsurprisingly, given the negligible PFT anomalies presented in Figure 5 for central Amazonia, most of the biome changes occur in northern, eastern, and southern Amazonia.

3.4.1 | Central Amazonia

Central Amazonia remains classified as humid evergreen tropical forests in all model combinations (0% of grid cells change to a mid-Holocene savannah classification, Figure 7b), despite the range of precipitation changes between the climate models (Figure 3, Figure 4b). The resilience of the central Amazonian humid evergreen tropical forests is a feature corroborated by the palaeo-data from this region (Figure 6; e.g. Colinvaux et al., 1996; Bush et al., 2000; Irion et al., 2006; Bush et al., 2007; Horbe et al., 2011).

TABLE 3 List of palaeoclimate sites. ID refers to location number in Figure 1b

ID	Site name	Lon. (°E)	Lat. (°N)	Proxy type	Reference(s)
1	SO147-106KL	−77.65	−12.05	Marine core erosion indicators (soil lithics)	Rein et al. (2005)
2	Cueva del Tigre/El Condor	−77.3	−5.94	Speleothem ($\delta^{18}O$ composition)	van Breukelen et al. (2008)/Cheng et al. (2013)
3	Shutuca Cave	−77.15	−5.12	Speleothem ($\delta^{18}O$ composition)	Bustamante et al. (2016)
4	Lake Junin/Huaguapo Cave	−75.9	−11.15	Lake calcite ($\delta^{18}O$ composition)/Speleothem ($\delta^{18}O$ composition)	Seltzer et al. (2000)/Kanner et al. (2013)
5	Lake Titicaca	−69.17	−16.17	Lake-level reconstruction (chemical and isotopic composition)	Baker et al. (2001), Rowe et al. (2002)
6	Sajama	−68.88	−18.1	Ice core (dust and snow accumulation	Thompson et al. (1998)
7	Laguna La Gaiba	−57.72	−17.76	Lake-level reconstruction (*Pediastrum*)	Whitney et al. (2011) Whitney and Mayle (2012)
8	Botuverá Cave	−49.16	−27.22	Speleothem ($\delta^{18}O$ composition, geochemical analysis)	Cruz et al. (2005), Wang et al. (2007), Bernal et al. (2016)
9	Santana Cave	−48.73	−24.53	Speleothem ($\delta^{18}O$ composition)	Cruz et al. (2006)
10	Lapa Grande	−44.37	−14.42	Speleothem ($\delta^{18}O$ composition)	Stríkis et al. (2011)
11	Lake Valencia	−67.75	10.17	Geochemistry and isotopic analysis	Bradbury et al. (1981), Curtis et al. (1999)
12	Cariaco Basin	−65.16	10.72	Marine core (Titanium and iron concentrations)	Haug et al. (2001)
13	Paraíso Cave	−55.45	−4.07	Speleothem ($\delta^{18}O$ composition)	Wang et al. (2017)
14	Rio Grande do Norte	−37.73	−5.6	Speleothem ($\delta^{18}O$ composition)	Cruz et al. (2009)

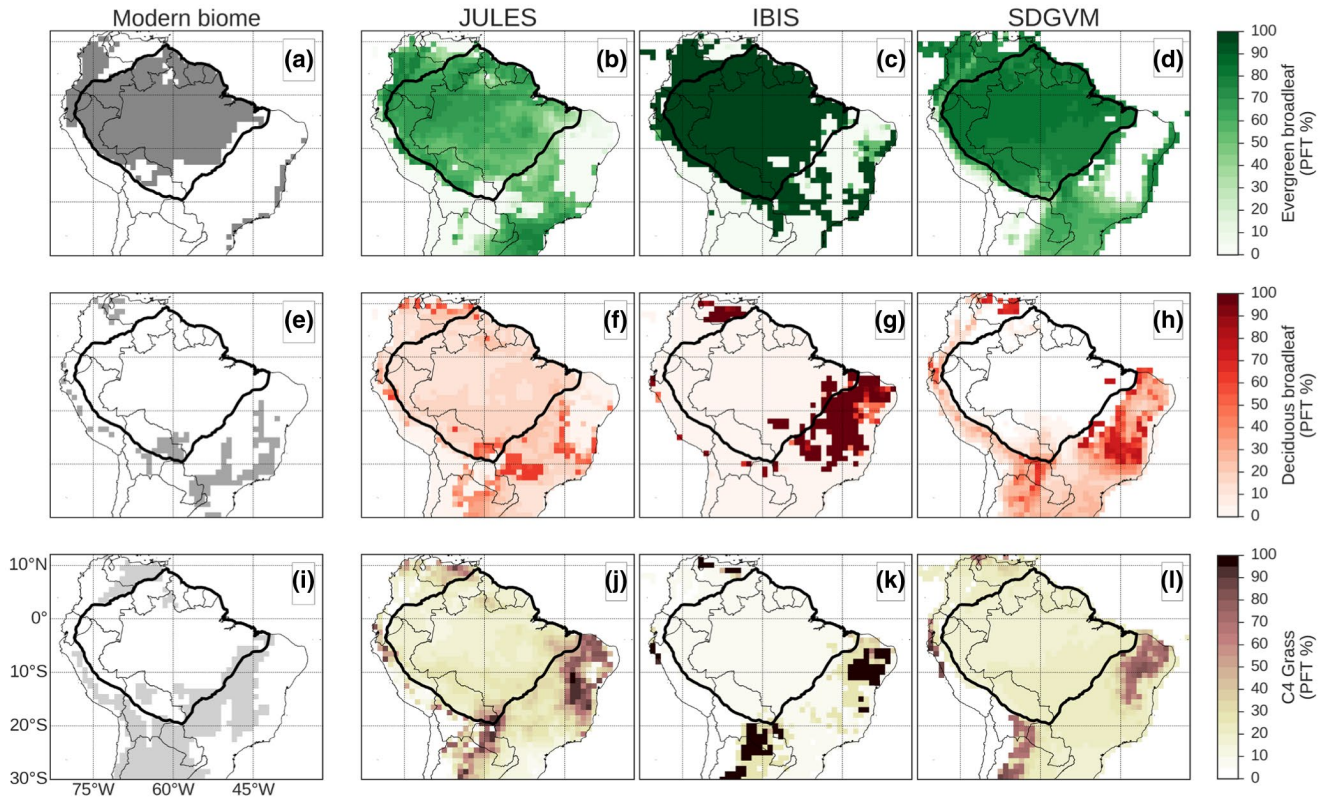

FIGURE 2 Modern distribution of potential broad ecoregions. (a) Humid evergreen tropical forest, (e) Semi-deciduous dry forest and (i) savannah/grassland (as in Figure 1), alongside simulated PFT distributions of evergreen broadleaf trees (b–d), deciduous broadleaf trees (f–h) and C4 grass (j–l) from the modern control runs of each vegetation model; JULES (b, f, j), IBIS (c,g,k) and SDGVM (d, h, l)

3.4.2 | Northern Amazonia

In northern Amazonia, extensive changes in biome classifications are seen in the simulations using the GISS-E2-R (Figure 6d–f); across all three DGVMs, ~20–25% more of the total grid cells in this region are classified as savannah in the mid-Holocene (Figure 7a). Biome changes in simulations using the other climate models are much less substantial, with only a few grid cells switching classifications between the mid-Holocene and modern control, apparently without a strong relationship with the magnitude or direction of precipitation changes (Figure 7a). Interestingly, SDGVM is the only vegetation model whose classification changes include grid cells switching to semi-deciduous tropical dry forest (e.g. under climates of FGOALS-s2, MIROC-ESM, and CSIRO-Mk3-6–0; Figure 6l,r,x, respectively). Unfortunately, there is a lack of suitable palaeodata records in this region for evaluation of these vegetation scenarios. Existing records do not extend back to the mid-Holocene (e.g. Charles-Dominique et al., 1998; Ledru, 2001; Montoya, Rull, Stansell, et al., 2011), reflect locally anomalous vegetation due to unusual geomorphology (e.g. Rull, 2004, 2005), or have been influenced by human activity to such an extent that the influence of past climate change upon vegetation is hard to discern (Rull et al., 2015).

3.4.3 | Eastern Amazonia

In eastern Amazonia, the available palaeoecological records show that there was some degree of mid-Holocene savannah expansion in ecotonal areas; for example, on the Serra Sul dos Carajás plateau (Table 2, id = 20; Absy et al., 1991; Hermanowski et al., 2012; Hermanowski et al., 2012; Sifeddine et al., 2001)at Lake Marabá (Table 2, id = 19; Guimarães et al., 2013), and at Lago do Saci (Table 2, id = 22; Fontes et al., 2017). However, the spatial extent of these savannah expansions is unclear from the palaeo-records, as these sites only have local-scale catchments, and in some cases (e.g. Carajas) may reflect ecotonal shifts atop inselbergs which may be unrepresentative of the surrounding lowlands below. Nevertheless, they provide a rough guide as to where we would expect biome changes in the mid-Holocene vegetation simulations.

In the JULES simulations, there is consistent savannah expansion along the eastern Amazonian ecotone in most of the climate models, despite their differences in precipitation anomalies. There is between a ~10 and 20% increase in the total grid cells classified as savannah in this region (Figure 7c). Spatially, this savannah expansion appears to match well with the palaeo-records in the north-east of the area, with grid cells to the east of Carajás/Marabá consistently switching to savannah. However, in the south-west of the area, the

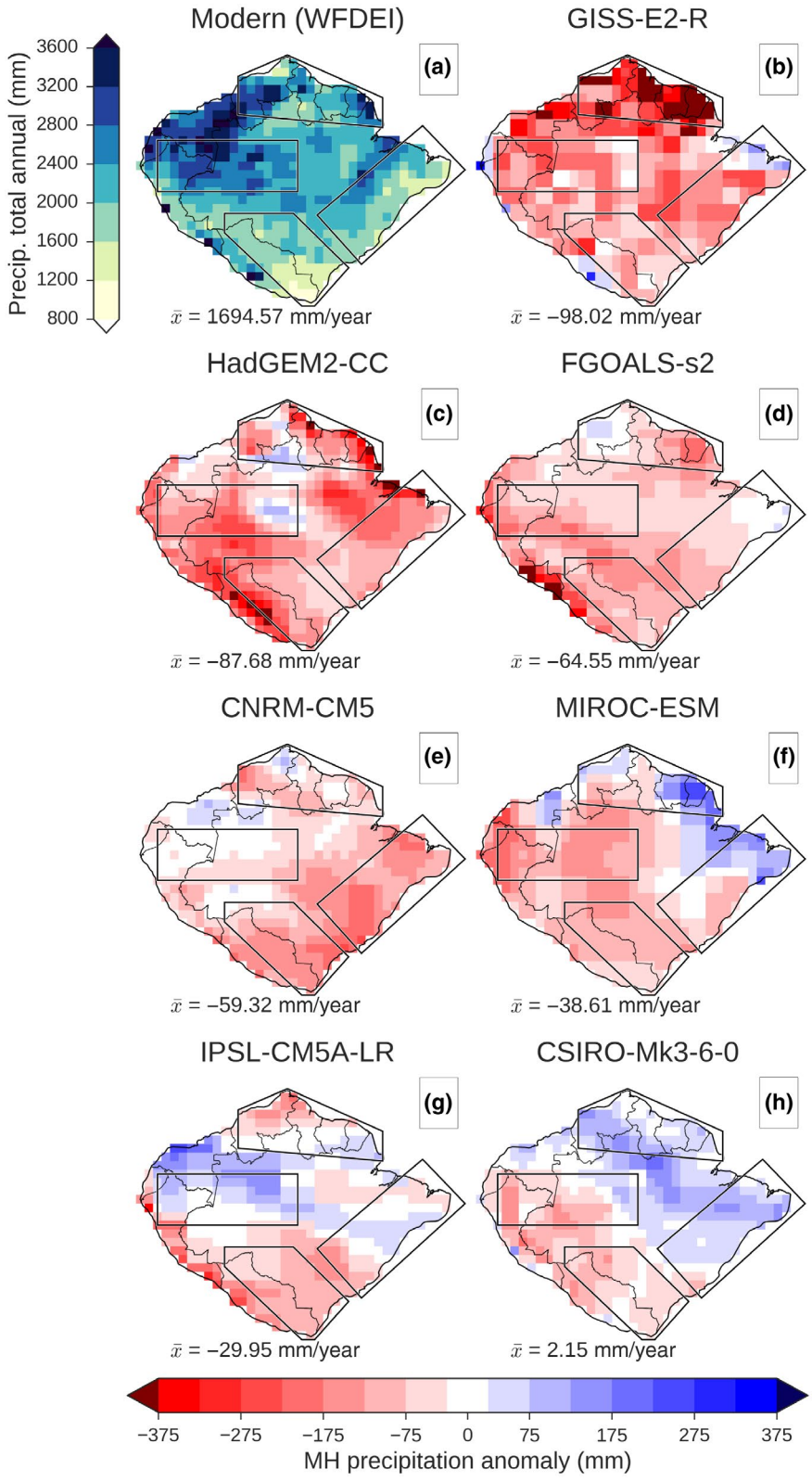

FIGURE 3 Mid-Holocene (MH) annual mean precipitation anomalies (mm/yr) from the prior CMIP5/PMIP3 climate models used in this study. Blue (red) corresponds to a wetter (drier) mid-Holocene compared with present day. Panel (a) presents the average annual precipitation from the WFDEI dataset to help put the changes in (b)–(h) into context. The value of $\bar{x}$ is the regional spatial mean. Polygons outline main areas of Amazonia, defined in Figure 1a

JULES savannah expansion does not reach Lago do Saci in any of the simulations. In the IBIS simulations, there is greater variation in biome classification changes between the climate models. The climate models with a drier mid-Holocene all show savannah expansion in eastern Amazonia (~5%–20%; Figure 7c), but the spatial distribution of this expansion varies. Under the two driest climate models, HadGEM2-CC and CNRM-CM5, grid cells switching to savannah are located all along the ecotone (Figure 6h,n), both in the north-east near Carajás/Marabá, and in the south-west, almost reaching Lago do Saci. Under GISS-E2-R and FGOALS-s2 (the next two driest climates), the savannah expansions are predominantly clustered in the south-west of eastern Amazonia (Figure 6e,k), in

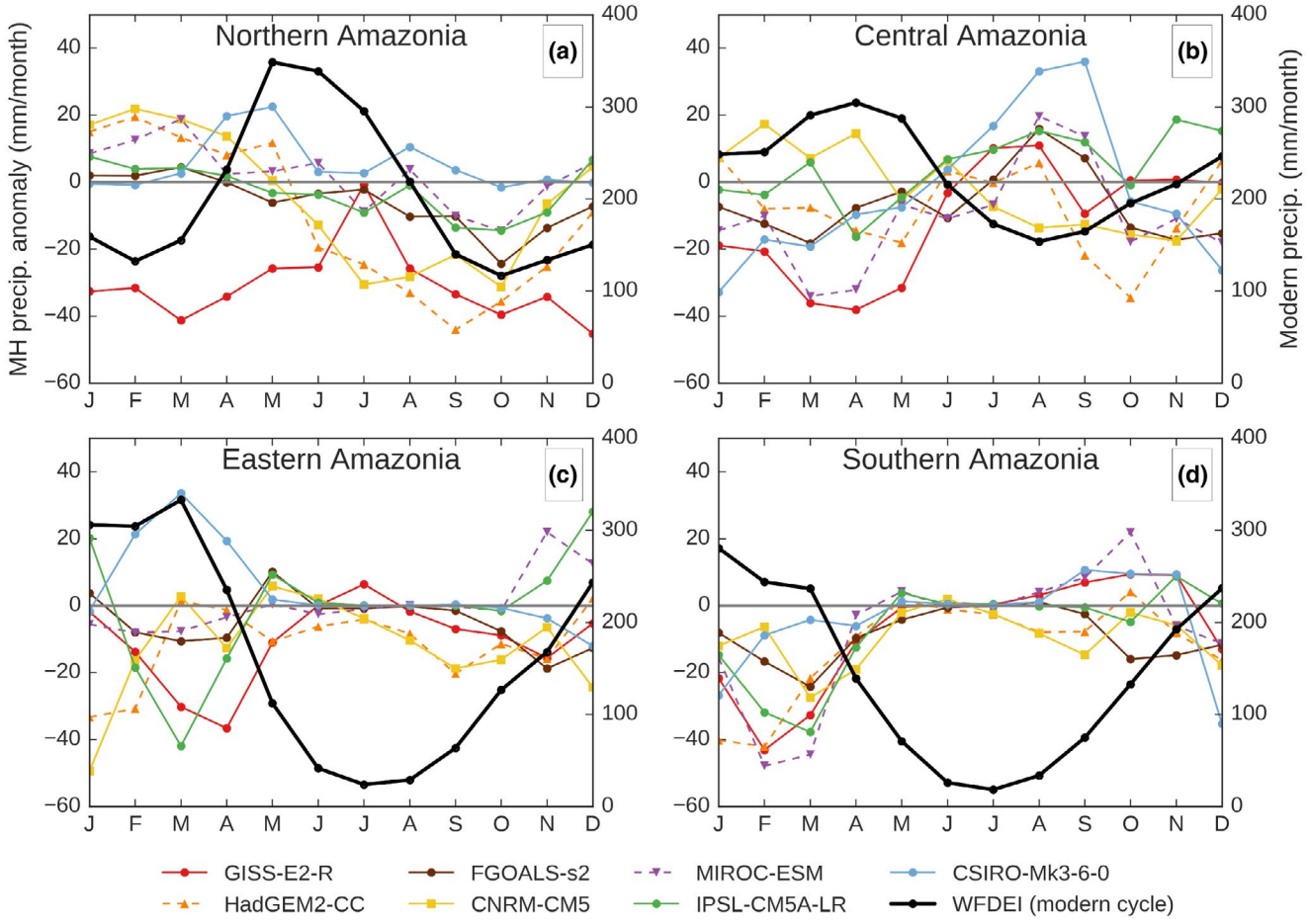

FIGURE 4 Average annual cycle of mid-Holocene (MH) precipitation anomalies (left hand y-axis) for each PMIP3 climate model used in this study for the four areas of Amazonia: (a) northern, (b) central, (c) eastern, and (d) southern (as defined in Figure 1a). The thick black line with black circles presents the average WFDEI modern precipitation annual cycle to help put the changes into context (right hand y-axis)

the grid cells surrounding Lago do Saci. In the SDGVM simulations, between ~10 and 20% grid cells change to savannah in the three driest climate models HadGEM2-CC, CNRM-CM5, and GISS-E2-R (Figure 7c). These changes occur predominantly in the north-east of the area near the Carajás/Marabá palaeo-records. Further into the Amazon basin in north-east Amazonia, under the HadGEM2-CC and CNRM-CM5 climates, SDGVM shows large patches of savannah centered at ~2°0′S, 54°0′W (Figure 6i,o). This does not match with the palaeo-records here; for example, Lago Tapajós (Table 2, id = 1; Irion et al., 2006) and the group of Prainha lakes (Table 2, id = 8; Bush et al., 2000; Bush et al., 2007), which show persistence of the humid evergreen tropical forests biome during the MH (e.g. Bush, Silman, & De Toledo, 2007; Irion et al., 2006). In the south of the area, as with JULES, savannah expansion in the SDGVM simulations does not reach Lago do Saci in any of the simulations.

With IBIS and SDGVM, simulations using the climate models that show a zero or positive mid-Holocene precipitation anomaly for eastern Amazonia (IPSL-CM5A-LR, MIROC-ESM, and CSIRO-Mk-3-6–0) generally show an increase in humid evergreen tropical forests grid cells, particularly in the north of the area. This is clearly at odds with the Carajás/Marabá palaeo-records, which show savannah expansion.

3.4.4 | Southern Amazonia

There is strong evidence from the palaeoecological data that southern Amazonia experienced significant vegetation changes during the mid-Holocene, compared with present. In north-eastern Bolivia, records from large lakes – Laguna Chaplin (Table 2, id = 6) and Bella Vista (Table 2, id = 5) – provide evidence that the southern Amazonian humid evergreen tropical forest ecotone was at least 130km further north than present (Burbridge et al., 2004; Mayle et al., 2000). To the north-west of these records, the large lake of Laguna Orícore (Table 2, id = 4) corroborates these findings (Carson et al., 2014). In the north/north-west of this southern Amazonia area, the extent of northward expansion of the ecotone is somewhat constrained by results from the soil pit profiles of Jaco Sa (Table 2, id = 34; Watling et al., 2017) which show persistence of rainforest during the mid-Holocene.

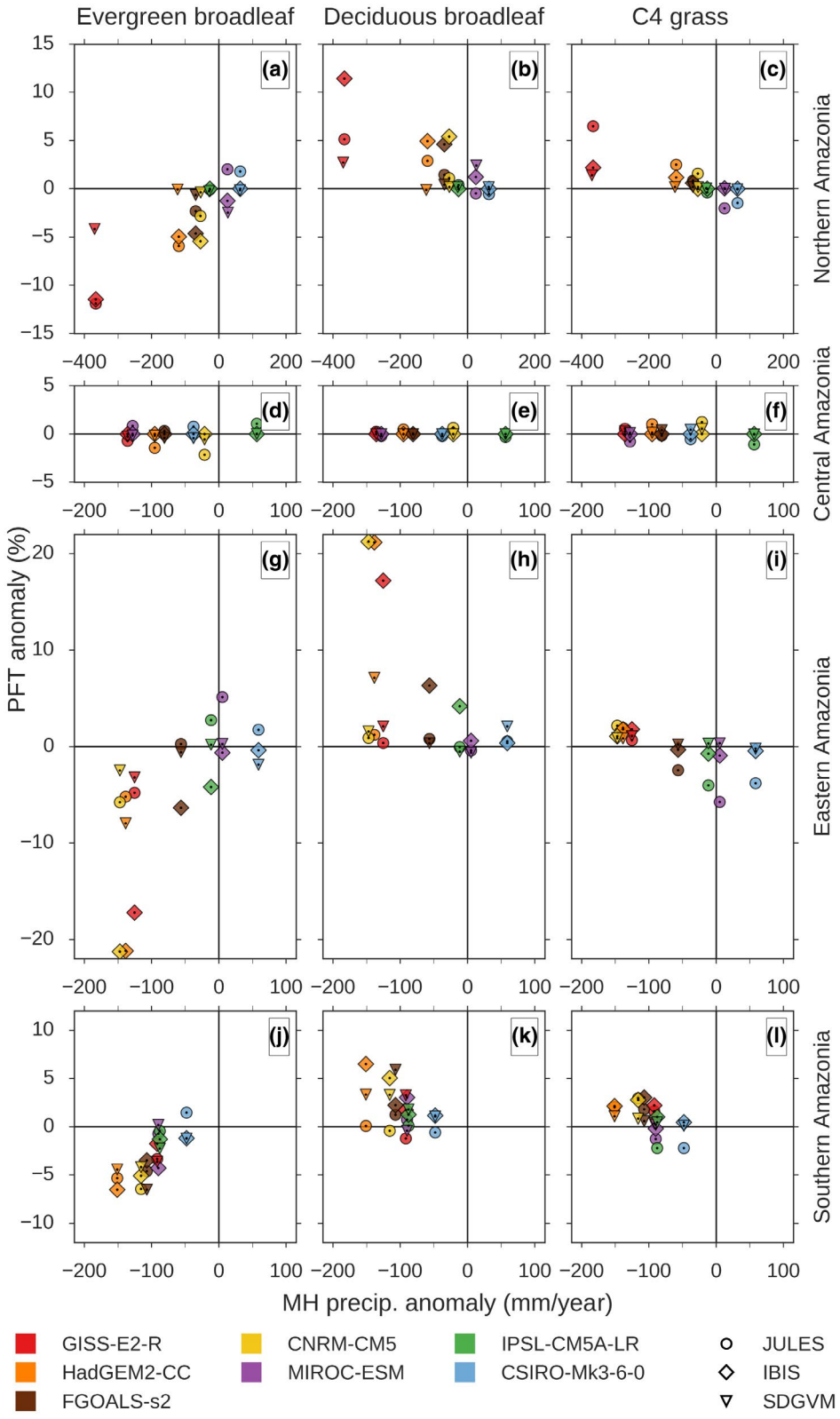

FIGURE 5 Mid-Holocene (MH) anomalies of the fractions for PFTs: evergreen broadleaf (a,d,g,j), deciduous broadleaf (b,e,h,k) and C4 grass (c,f,i,l), plotted against annual precipitation anomaly for each given climate model. Averaged for the four areas of Amazonia: northern (a–c), central (d–f), eastern (g–i), and southern (j-l) (as defined in Figure 1a)

In the JULES simulations, all climate model runs show some degree of savannah expansion in this area, with between 15 and 30% of grid cells switching to savannah (Figure 7d). The extent of this expansion appears to be roughly related to the degree of drying in the climate models, the drier climate models having more grid cells switching to savannah. The spatial distribution of savannah expansion in JULES

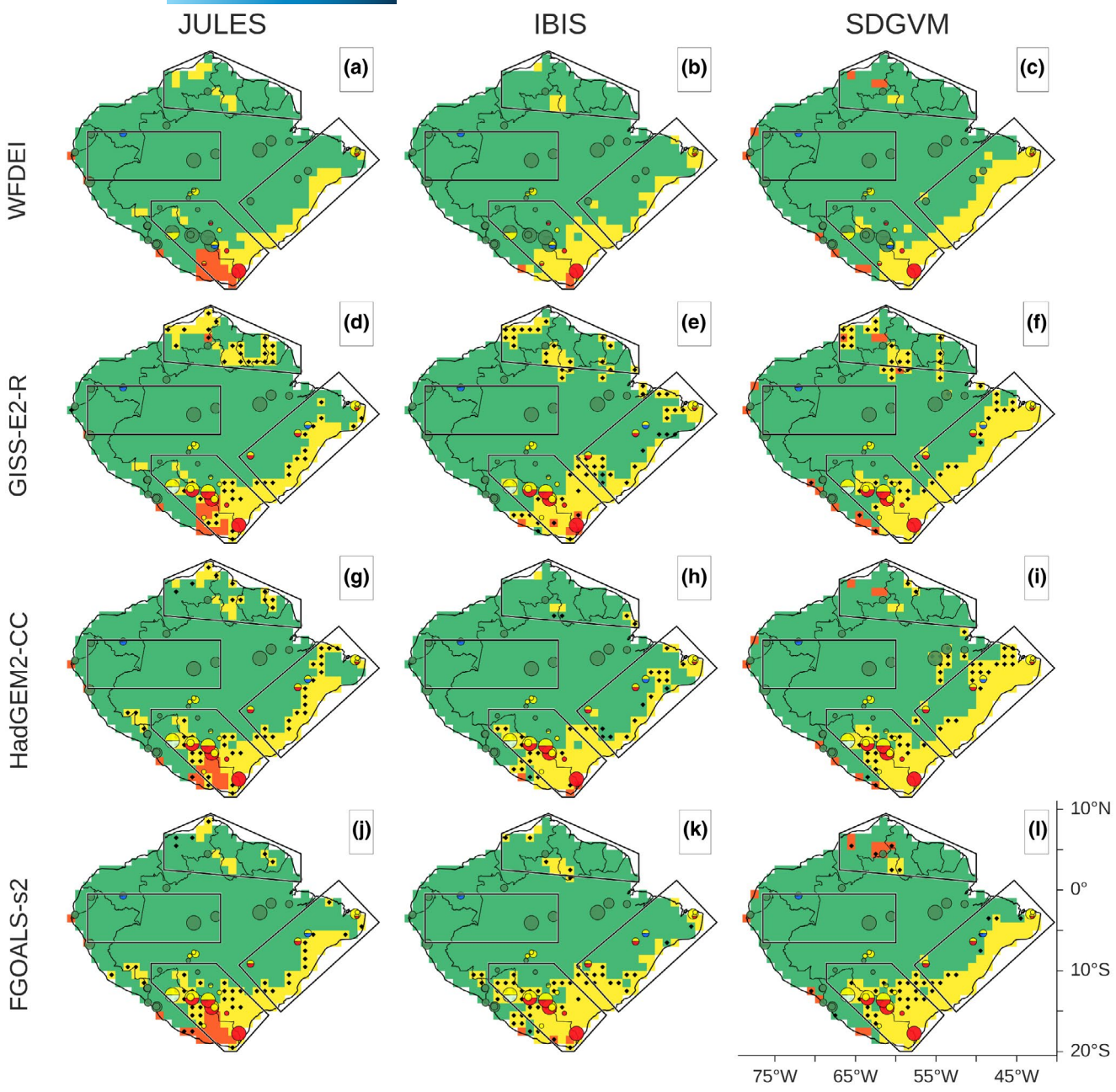

FIGURE 6 Results of the LDA vegetation classification, overlaid with palaeoecological data reconstructions. (a–c) Modern control simulations. (d–x) Mid-Holocene simulations, where black dots represent grid cells where the LDA vegetation classification is different between the mid-Holocene and modern control. Polygons outline the main sub-divisions of Amazonia, defined in Figure 1a. In the palaeodata symbols, the pale blue indicates gallery forest and the dark blue indicates palm swamp. Green palaeodata symbols and model grid cells represent humid evergreen tropical forest, red symbols represent semi-deciduous dry forest, and yellow symbols represent savannah/grassland/shrubland

appears to compare well with the palaeo-records, with most climate models showing increased savannah classifications through north-east Bolivia up to Laguna Orícore. Some isolated grid cells switch to savannah further north (e.g. in HadGEM2-CC, FGOALS-s2, and MIROC-ESM; Figure 6g,j,p), but never as far as, for example, the Jaco Sa palaeo-records from eastern Acre. Results from the IBIS simulations are more varied than those from JULES. The drier climate models of HadGEM2-CC and FGOALS-s2 produce savannah expansion at a similar level to JULES (~20%–30% grid cells switch), though the second driest climate model in this area, CNRM-CM5, appears to be a slight outlier, with only ~12% of grid cells switching to savannah (Figure 7d). The remaining climate models show <10% savannah expansion in this area, even though they all simulate a drier mid-Holocene climate. IPSL-CM5A-LR and CSIRO-Mk3-6-0 even have a few grid cells that switch to humid evergreen tropical forests in north-east Bolivia near the palaeo-record of Laguna Chaplin. In the SDGVM simulations, results from the driest three climate models (HadGEM2-CC, CNRM-CM5, and FGOALS-s2) match closely with

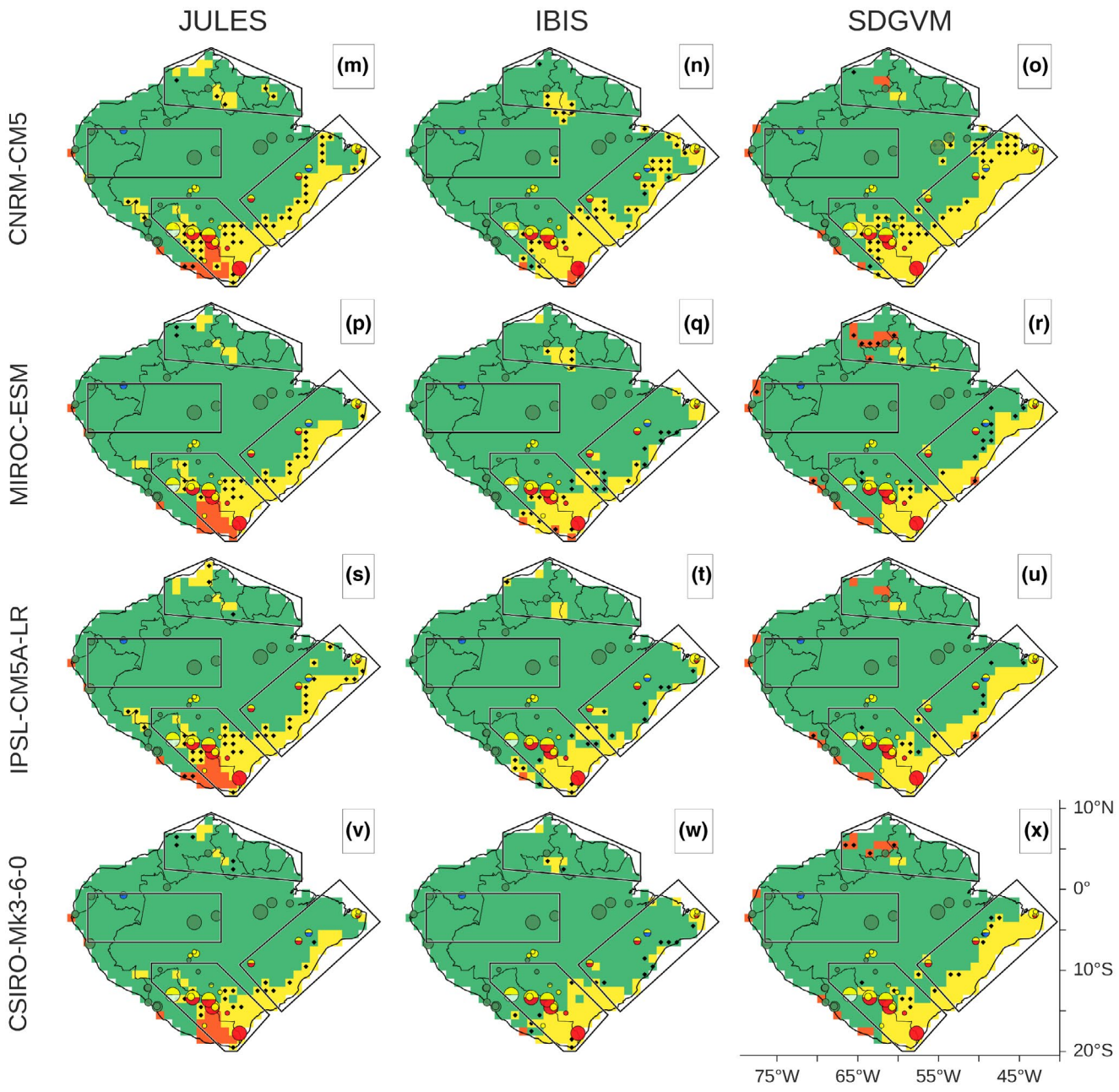

FIGURE 6 (Continued)

those of JULES, both in terms of magnitude of grid cell changes (~25%–30%; Figure 7d) and the spatial distribution of these changes. Conversely, the remaining climate models show more agreement with the IBIS simulations, with much less savannah expansion across the area.

Given the relatively high density of palaeodata in southern Amazonia, the level of model-palaeodata agreement in this region can be quantified at the locations of the palaeodata and summarized using the Cohen's Kappa statistic (Cohen, 1960) for each climate-DGVM model configuration (Figure 8). In Figure 8, the climate models are ordered from those with the largest drying at the top to those with the least drying at the bottom. The LDA classifications driven by climate models that simulate −100 to −150 mm per year precipitation change (drying) in southern Amazonia display the highest κ-values, indicating a better level of agreement between the models and palaeodata. These results suggest that JULES is highly sensitive to decreases of precipitation in southern Amazonia, which is perhaps what one would expect, given the climatically sensitive nature of this region, whereas in IBIS and SDGVM, there appears to be a threshold of ~100 mm decrease in annual precipitation needed to initiate the level of savannah expansion shown by the palaeo-records. In general, JULES has a higher level of agreement with the palaeodata than the other DGVMs, under all climate model forcings.

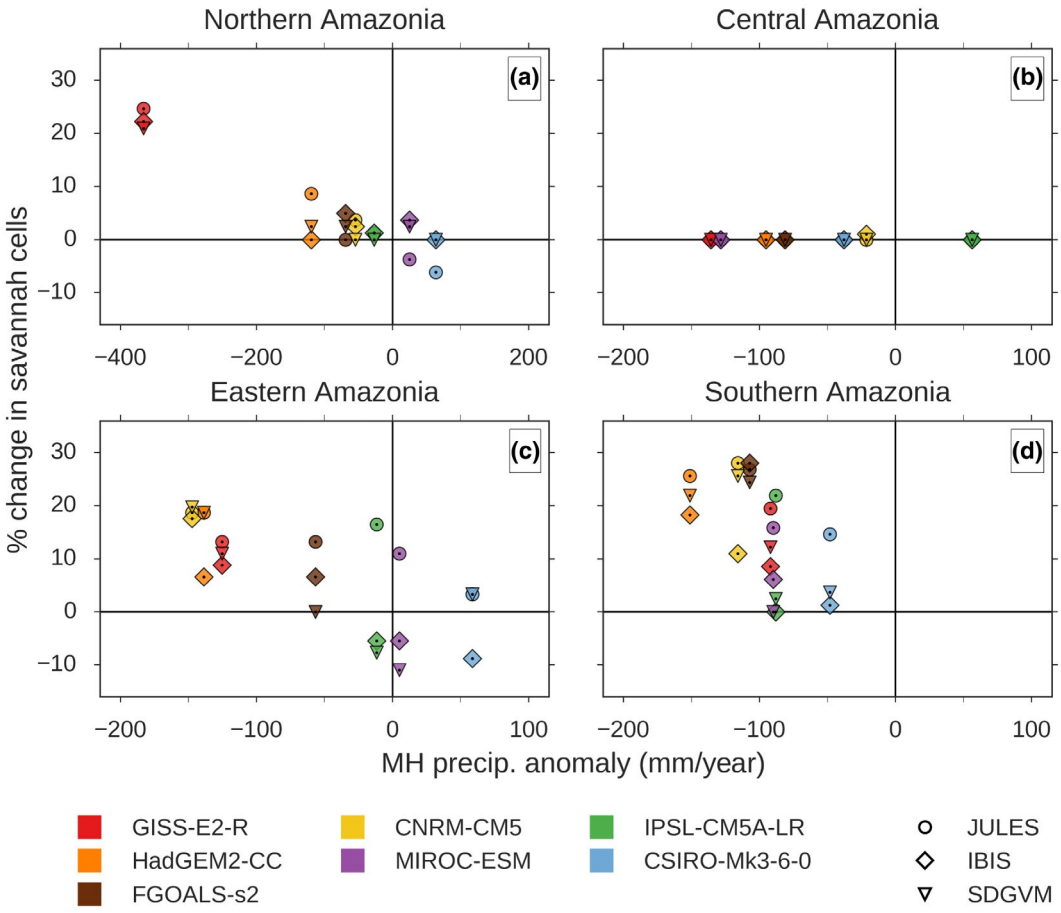

FIGURE 7 Percentage change in the proportion of savannah cells (based on the LDA classification). Percentage change is relative to total cells between the mid-Holocene (MH) and modern control for each of the areas of Amazonia: (a) northern, (b) central, (c) eastern, and (d) southern (as defined in Figure 1a)

4 | DISCUSSION

4.1 | Assessment of the overall scale of Amazon rainforest dieback resulting from mid-Holocene drying

4.1.1 | Central Amazonia

The central and western areas of Amazonia are presently some of the wettest parts of tropical South America (> ~2500–3000 mm/yr; Figure 1b), with relatively consistent levels of precipitation throughout the year (Figure 4b). Speleothem records from the Peruvian Amazon (i.e. Cueva del Tigre/El Condor – Table 3, id = 2, Shutuca Cave – Table 3, id = 3) provide evidence that western Amazonia was moderately drier than present during the mid-Holocene, though the magnitude of drying is difficult to quantify based on these records alone. Generally, all climate models show some degree of mid-Holocene drying in this region, but in no climate model's mid-Holocene simulation does annual precipitation decrease by >300 mm in any central Amazonian grid cell (Figure 3), with the average annual anomaly across the whole central Amazonian area ranging from +55 mm/yr (IPSL-CM5A-LR) to −140 mm/yr (GISS-E2-R).

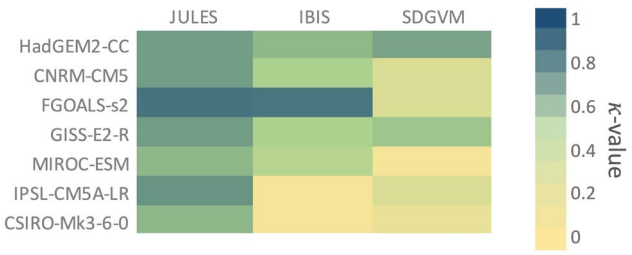

FIGURE 8 Heatmap of the level of agreement between modelled LDA mid-Holocene vegetation classification and palaeodata vegetation classification. Heatmap values were calculated using the Cohen's Kappa statistic (κ-value; Cohen, 1960)

Therefore, given that humid evergreen tropical forest is supported in climates > ~1600 mm/yr (Malhi & Wright, 2004), we would not expect there to be any biome-scale turnover in this area based on precipitation changes alone. It is reassuring then, that all our DGVM simulations show that, on a biome scale, the core of the Amazonian humid evergreen rainforest was unchanged with any scenario of mid-Holocene climate change (Figures 5, 6, 7b). This finding is consistent with the relatively sparse palaeoecological records from this

region, which show persistence of rainforest vegetation through the mid- to late-Holocene (Smith & Mayle, 2018). However, we note that these palaeo-records are predominantly from small basins (e.g. Behling et al., 1999; Bush & Colinvaux, 1988; Bush et al., 2004), which only reveal local-scale vegetation histories. Our simulations therefore provide important supporting evidence that the humid evergreen tropical forests biome was resilient across the whole of central Amazonia, not just in the local catchments of small, sparse palaeoecological sites.

4.1.2 | Northern Amazonia

In northern Amazonia, only the DGVM simulations forced with the GISS-E2-R climate predict large-scale savannah expansion during the mid-Holocene (Figure 6d–f). The northern Amazonian mid-Holocene precipitation simulation from GISS-E2-R is a notable outlier compared with the other climate models, simulating a substantially drier mid-Holocene climate across the whole area (~375 mm/yr decrease on average). Although there are no palaeo-precipitation records from directly within this area, evidence from other palaeo-precipitation records in the northern hemisphere of tropical South America (i.e. Lake Valencia – Table 3, id = 11, Cariaco Basin – Table 3, id = 12) suggest this level of mid-Holocene drying is unlikely. Therefore, only considering DGVM simulations forced using the other climate models, the results suggest overall humid evergreen tropical forest stability in this area. Some small differences are noted between these simulations, with a range of between −8 and +5% change in the number of savannah grid cells (Figure 7a). These changes do not appear to be consistent between the three DGVMs, even when using the same climate model (suggesting uncertainty between the DGVMs). Spatially, these differences occur mainly around the Gran Sabana/Roraima savannah in northern Brazil, a notoriously difficult area to understand the underlying drivers of long-term vegetation dynamics, given the complexity of human, edaphic, fire, and climatic factors that influence this savanna vegetation (Montoya & Rull, 2011; Montoya et al., 2011; Rull et al., 2015). Therefore, the differences in the models are likely a result of the difficulty in the DGVMs modelling this area of savannah, and/or the difficulty in the LDA algorithm classifying these grid cells.

4.1.3 | Eastern Amazonia

In contrast to central and northern Amazonia, there is more uncertainty regarding the mid-Holocene dieback of humid evergreen tropical forests in eastern Amazonia, with a range between the different model simulations in the direction, magnitude, and spatial extent of any biome changes. The simulated changes in savannah extent do appear to be, at least in part, related to the different precipitation regimes in the different climate models; drier climates tend to cause more savannah expansion in all three DGVMs (Figure 7c). This finding is pertinent, given the debate in the palaeo-community surrounding the mid-Holocene precipitation history of eastern Amazonia. The savannah and dry forest expansion at the palaeoecological sites on the Carajás plateau (Table 2, id = 20) and at Lago do Saci (Table 2, id = 22) suggest drier mid-Holocene conditions in eastern Amazonia, supporting the hypothesis of a weaker SASM due to a decrease in austral summer insolation (Absy et al., 1991; Fontes et al., 2017; Hermanowski, Costa, & Behling, 2012; Hermanowski, da Costa, Carvalho, et al., 2012; Sifeddine et al., 2001). However, the recent speleothem record from Paraíso Cave (Table 2, id = 13) contrasts with these interpretations, whereby more negative $\delta^{18}O$ values point to a wetter-than-present mid-Holocene in the eastern Amazonia region (Cheng et al., 2013; Wang et al., 2017). Even though this speleothem site is not within our defined area of eastern Amazonia, it is likely that its palaeoclimate record is representative of at least the northern part of our defined 'Eastern Amazonia' area, given that the climate around the Paraíso Cave is influenced predominantly by easterly winds originating from the tropical Atlantic (Wang et al., 2017).

Using climate models with a wetter mid-Holocene eastern Amazonia (CSIRO-Mk3-6-0, IPSL-CM5A-LR, MIROC-ESM; Figure 3), in concordance with the Paraíso Cave palaeodata, our DGVM simulations generally show humid evergreen tropical forest expansion along the eastern Amazonian ecotone. Given the palaeoecological evidence of savannah expansion, we suggest that these simulation results are unlikely, and that the Paraíso Cave record may not be representative of the eastern Amazonian ecotone. Fontes et al. (2017) explore some potential mechanisms that might explain this apparent mismatch between the Paraíso speleothem record and palaeoecological data, such as decreased extent of Amazonian rainforest influencing the atmospheric $\delta^{18}O$ through a reduction in moisture recycling via evapotranspiration, and/or increased precipitation in north-east Brazil (e.g. Rio Grande do Norte, Figure 1b, id = 14; Cheng et al., 2013) propagating a negative $\delta^{18}O$ anomaly westward into eastern Amazonia. Nevertheless, given the paucity of palaeorecords and the uncertainty between the model simulations, it is difficult to definitively rule out any scenarios of mid-Holocene precipitation/vegetation changes in eastern Amazonia. There is a clear need for more palaeoecological and palaeoclimate records from this sector of the basin to improve understanding of the nature of mid-Holocene vegetation–climate relationships in Amazonia.

4.1.4 | Southern Amazonia

The strongest agreement between model simulations and palaeodata is found in southern Amazonia, where there is clear evidence for the vulnerability of ecotonal Amazonian humid evergreen tropical forests to mid-Holocene drought (Figure 8). With an annual precipitation of ~1500–2000 mm/yr (Figure 1b) and a long, 5–7 month, dry season (Figure 4d), this region is at the climatic threshold of supporting humid evergreen tropical forests (Malhi et al., 2009; Malhi & Wright, 2004). Therefore, even a relatively small decrease in precipitation would be expected to cause some degree of rainforest dieback

in this region. All of the climate models simulate a drier-than-present mid-Holocene for southern Amazonia, which is corroborated by the independent palaeoclimate records from the Bolivian/Peruvian Andes (Table 3, ids = 4–6) and lowland eastern Bolivia (i.e. Laguna La Gaiba, Table 3, id = 7). Consequently, most of the DGVM simulations show some degree of humid evergreen tropical forest dieback (Figure 5j) and expansion of savannah grid cells in the subsequent LDA classifications (Figure 7d).

The relative abundance of palaeoecological records in southern Amazonia allows us to assess the skill of our simulations and LDA classifications with more confidence than in the other areas of Amazonia. The savannah/dry forest expansion along the border of north-eastern Bolivia and adjacent Brazil, as shown through the regional-scale vegetation reconstructions from Laguna Chaplin, Bella Vista, and Orícore is a relatively consistent feature among all three DGVMs driven with the driest three climate models in this area. However, under the climate models with less precipitation decrease, only JULES reproduces the expected savannah expansion in eastern Bolivia, with IBIS and SDGVM showing negligible changes in biome classifications. Given the quantified levels of model-data agreement displayed in Figure 8, we have more confidence in the drier climate models (HadGEM2-CC, CNRM-CM5, and FGOALS-s2) to simulate mid-Holocene vegetation changes in southern Amazonia, given that all DGVMs show the expected savannah expansion under these drier climate scenarios. These models which simulate a drier mid-Holocene for southern Amazonia also share positive temperature anomalies for this region (Figure S4.2), which, although small, further push the models towards the threshold for rainforest dieback (consistent with the findings by Good et al., 2011, for future projections).

Despite southern Amazonia having more palaeoecological records than the other areas of Amazonia, there are still insufficient sites to precisely constrain the scale of the northward shift of the humid evergreen tropical forest ecotone. Currently, the farthest north this shift has been detected on a large scale is at Laguna Orícore (Carson et al., 2014). There is some evidence for small, localized patches of savannah expansion occurring at small 'savannah islands' within the dense humid evergreen tropical forests, ~500 km north of Orícore, though the expanded savannah islands were still likely surrounded by humid evergreen tropical forests (Table 2, ids = 31–33; de Freitas et al., 2001; Pessenda et al., 2001). In eastern Acre, the Jaco Sa soil profiles (Table 2, id = 34) provide evidence that the bamboo forest ecosystem that exists there today was present during the mid-Holocene (Watling et al., 2017), suggesting that the northerly shift of the humid evergreen tropical forest-savannah ecotone did not extend to this region. However, there are as yet no palaeo-records to determine the extent of mid-Holocene rainforest extent in the region between Orícore and Jaco Sa.

In the model simulations that show reasonable agreement with the palaeo-data (i.e. the three DGVMs using the climates of HadGEM2-CC, CNRM-CM5, and FGOALS-s2), the spatial extent of savannah expansion appears to be limited to the region around Laguna Orícore, extending into the Brazilian state of Rondônia north of Orícore by one or two grid cells (Figure 6), with only one exception of IBIS forced with FGOALS-s2 climate (Figure 6k). Overall, our model simulation results suggest that the northern Bolivian humid evergreen tropical forest was largely unaltered during the mid-Holocene, with the area around Laguna Orícore most likely the northernmost extent of savannah expansion. Savannah expansion is also a feature of these simulations in the eastern part of southern Amazonia (south-west Mata Gross state, Brazil). However, this area is mostly savannah in the present day (Figure 1a), so mid-Holocene savannah 'expansion' here is partly a result of the modern ecotone being slightly too far south in the DGVM simulations.

While the climate model and DGVM combinations display different magnitudes of precipitation decrease and savannah expansion, there is a strong relationship between the two (Figure 3d), suggesting common mechanisms are involved in the model responses. A linear regression of savannah-area-change against precipitation change enables the quantification of the sensitivity of the forested area to long-term drought. In southern Amazonia, the regression ($R^2 = 0.77$) suggests that for each 100 mm decrease in precipitation there would be a savannah expansion of ~125,000 km^2, which effectively equates to tropical forest loss (humid evergreen tropical forests and semi-deciduous tropical dry forest) of the same magnitude. Given that the model combinations which produce a higher level of agreement with the palaeodata display 100–150 mm decrease in precipitation, this would suggest a scale of tropical forest dieback during the mid-Holocene of 125,000–185,000 km^2, or an area at least the size of England from southern Amazonia alone.

4.2 | Implications for understanding future Amazonian ecosystem change

Early modelling studies predicted that future climate change could trigger large-scale Amazonian Forest dieback (e.g. Betts et al., 2004; Cox et al., 2000, 2004; Huntingford et al., 2008). Although more recent simulations have demonstrated much less rainforest dieback (e.g. Good et al., 2013; Huntingford et al., 2013), varying amounts of loss across Amazonia are still seen in simulations using different DGVMs (e.g. Sitch et al., 2008) and climate models (e.g. Malhi et al., 2009). In our multi-model study, the central Amazonian humid evergreen tropical forest biome is stable in all of our mid-Holocene model simulations and this finding is verified by the available palaeoecological data. The lack of impact in central Amazonia may be a cause for hope regarding the future of the region, as our results give support to the projections where the core of Amazonia remains largely forested under drier climatic conditions, although rapid deforestation rates in this region should curb this optimism. Our mid-Holocene simulations also add weight to evidence from other modelling and ecological studies (e.g. Allen et al., 2017; Cook et al., 2012; Fisher et al., 2007; Malhi et al., 2009) that the transitional, ecotonal forests of eastern and southern Amazonia will be especially vulnerable to future drought and may experience significant forest dieback. We have used the mid-Holocene multi-model response to provide a rough baseline sensitivity of tropical forest to declining

rainfall. Our results suggest an area of 125,000 km^2 of tropical forests in southern Amazonia would be lost for every 100 mm decrease in annual rainfall, all other factors being equal. The CMIP5 high emissions scenario (representative concentration pathway, RCP 8.5) produces an average decrease in rainfall over Amazonia that is similar in magnitude to the mid-Holocene drying, suggesting a loss of tropical forest the area of England by the end of the century. The southern and eastern parts of Amazonia were found to be more sensitive to rainfall decline than other areas, and are likely closer to the threshold for dieback, as previously found by Good et al. (2011).

The approach taken in this study, of creating an ensemble of simulations using three DGVMs, each driven by seven climate models, allows us to explore the uncertainties in the palaeo simulations and potentially to constrain the uncertainties in future projections. The climate models with drier mid-Holocene anomalies (HadGEM2-CC, CNRM-CM5, and FGOALS-s2) in southern Amazonia generally produce better agreement with the palaeoecological data. These models also have the most evident dipole in precipitation change across tropical South America between wetter conditions over the Nordeste region of Brazil and drier conditions across southern Amazonia and the north coast over Guyana (see Figure S4.3). In those models displaying this spatial pattern, it is related to a southward shift of the Atlantic Oceanic ITCZ (mechanism described in Singarayer et al., 2017), and these models also have a similar common dipole pattern and ITCZ shift in climate projections under the RCP8.5 scenario (Schmidt, Annan, et al., 2014). It is a notably different response pattern to the models that do not have a strong mid-Holocene dipole and poorer model-data agreement (e.g. GISS-E2-R, CSIRO-Mk3-6-0), and could indicate that a dipole response is more likely in the future. Models that produce the better matches to the palaeoecological data in southern Amazonia (Figure 8) also tend to be drier in both the mid-Holocene and RCP8.5 scenarios than other models. This indicates that we may expect a greater risk of drought-induced forest dieback than the ensemble average suggests.

The mid-Holocene represents an approximate analogue for future projected drying and has potential to contribute to narrowing uncertainties in future predicted rainfall changes, which display little model agreement at the present time. Key to this is the compilation of palaeodata from regions that would help to constrain the models. Currently, the majority of direct evidence of climate change comes from speleothem records or lakes in the high Andes or across southern Brazil. There is a need for more independent palaeoclimate records to be collected from across the Amazonian lowlands, although the scarcity of limestone bedrock in Amazonia means that speleothem-based palaeoclimate records will inevitably be rare in the core of the basin. There is also a clear need for transects of additional sites spanning the humid evergreen tropical forest/savannah ecotones across southern and eastern Amazonia to constrain the magnitude of the ecotonal shifts towards the margins of the Amazon basin, although suitably old lakes needed for pollen-based mid-Holocene vegetation reconstructions are rare.

While the use of mid-Holocene climate scenarios in this study has given important insights into the baseline sensitivity of tropical forests across Amazonia to changing precipitation regimes, there are other factors that will be important over the course of this century, most notably temperature, atmospheric CO_2 concentrations, and anthropogenic land use – especially the use of fire. Between the mid-Holocene and pre-industrial, both temperature (Figure S4.2) and CO_2 changes were relatively small, so precipitation decrease was by far the largest factor in producing mid-Holocene tropical forest dieback. Increased temperatures in future scenarios may exacerbate dieback by enhancing evapotranspiration and reducing photosynthetic rates (Galbraith et al., 2010; Schaphoff et al., 2006; Zhang et al., 2015), though some argue that tropical forests have some inherent resilience to direct effects of temperature increases (Lloyd & Farquhar, 2008). The effect of rising atmospheric CO_2 levels may help mitigate against dieback through the 'CO_2 fertilization' effect, although there is debate about how significant this process will be (Galbraith et al., 2010; Lapola et al., 2009; Rammig et al., 2010). Additionally, plants use less water under higher CO_2 levels due to reduced stomatal conductance, and this may lower sensitivity of ecotonal tropical forests to rainfall decrease. Conversely, the resulting reduction in transpiration could actually exacerbate drought by reducing atmospheric convective activity (Langenbrunner et al., 2019; Swann et al., 2016). Good et al. (2011) explored the combined, effects of temperature, precipitation, and CO_2 on tropical forests and found that enhanced CO_2 fertilization approximately balances out any negative impact from warming and increased drought.

Of most obvious concern is the impact of direct anthropogenic land use (i.e. deforestation, forest fragmentation, and fire use), most of which occurs in the ecotonal areas of eastern and southern Amazonia (the 'arc of deforestation'). Deforestation itself could cause considerable precipitation decreases through reduced atmospheric moisture recycling, crossing a tipping point that could make forest regrowth difficult (Boers et al., 2017; Shukla et al., 1990). The latter would likely be compounded by the 'edge effect' of forest fragmentation leading to further drying of forest patches (e.g. Ewers & Banks-Leite, 2013). We have shown that the southern and eastern ecotone regions are already sensitive to precipitation changes, with dry mid-Holocene climate scenarios causing expansion of savannah at the expense of rainforest. The additional anthropogenic pressures of deforestation and fire-use will only serve to exacerbate any climate-driven ecotonal shifts we might expect in these areas in the future (e.g. Barlow et al., 2020). In particular, the effect of a future drier climate increasing the likelihood of small-scale anthropogenic fires escaping into uncontrollable wildfires (a worrying phenomenon in recent dry years) is perhaps the greatest cause of concern for the future of Amazonia's forests. Incorporating fire into the next generation of Earth System models undoubtedly represents an important challenge for the modelling community.

ACKNOWLEDGEMENTS

We thank David Beerling and Lyla Taylor (University of Sheffield) for providing the SDGVM source code. JULES source code was accessed through the Met Office Science Repository Service (MOSRS). IBIS source code was accessed through the Center for Sustainability

and the Global Environment, University of Wisconsin-Madison. RS was funded by the UK Natural Environment Research Council (NERC) 'SCENARIO' Doctoral Training PhD award (2014–2018): NE/L002566/1. We thank Chris Jones and another reviewer, whose comments and suggestions greatly improved the manuscript.

CONFLICT OF INTEREST

The authors have no conflict of interest to declare. All co-authors have seen and agree with the contents of the manuscript and there is no financial interest to report. We certify that the submission is original work and is not under review at any other publication.

AUTHORS' CONTRIBUTIONS

JS and FM conceived and designed the overall project and supervised PhD student RS, who undertook the modelling analyses and palaeo-data compilation and wrote the first draft of the paper. All authors contributed to interpretation of the results and subsequent drafts of the paper. JS and FM provided the guidance to RS on modelling and palaeo-data synthesis/interpretation, respectively. JS performed the corrections and additional analyses following review.

DATA AVAILABILITY STATEMENT

The PMIP3 climate model data that were used in this study are publicly available at: https://esgf-node.llnl.gov/projects/esgf-llnl/. The dynamic vegetation model data that support the findings of this study are available from the corresponding author upon reasonable request.

ORCID

Richard J. Smith https://orcid.org/0000-0002-6447-6740
Joy S. Singarayer https://orcid.org/0000-0002-1504-1193
Francis E. Mayle https://orcid.org/0000-0001-9208-0519

REFERENCES

Absy, M. L., Cleef, A., Fournier, M., Martin, L., Servant, M., Sifeddine, A., Ferreira da Silva, M. F., Soubies, F., Suguio, K., Turcq, B., & Van der Hammen, T. (1991). Mise en évidence de quatre phases d'ouverture de la forêt dense dans le Sud-Est de l'Amazonie au cours des 60 000 dernières années: Première comparaison avec d'autres régions tropicales. *Comptes Rendus De L"académie Des Sciences. Série 2, Mécanique, Physique, Chimie, Sciences De L"univers. Sciences De La Terre*, *312*, 673–678.

Allen, K., Dupuy, J. M., Gei, M. G., Hulshof, C., Medvigy, D., Pizano, C., Salgado-Negret, B., Smith, C. M., Trierweiler, A., Van Bloem, S. J., Waring, B. G., Xu, X., & Powers, J. S. (2017). Will seasonally dry tropical forests be sensitive or resistant to future changes in rainfall regimes? *Environmental Research Letters*, *12*(2), 023001. https://doi.org/10.1088/1748-9326/aa5968

Aragão, L. E. O. C., Poulter, B., Barlow, J. B., Anderson, L. O., Malhi, Y., Saatchi, S., Phillips, O. L., & Gloor, E. (2014). Environmental change and the carbon balance of Amazonian forests. *Biological Reviews*, *89*, 913–931.

Baker, P. A., & Fritz, S. C. (2015). Nature and causes of Quaternary climate variation of tropical South America. *Quaternary Science Reviews*, *124*, 31–47.

Baker, P. A., Seltzer, G. O., Fritz, S. C., Dunbar, R. B., Grove, M. J., Tapia, P. M., Cross, S. L., Rowe, H. D., & Broda, J. P. (2001). The history of South American tropical precipitation for the past 25,000 years. *Science*, *291*, 640–643. https://doi.org/10.1126/science.291.5504.640

Bao, Q., Lin, P., Zhou, T., Liu, Y., Yu, Y., Wu, G., & He, B. (2013). The flexible global ocean-atmosphere-land system model, spectral version 2: FGOALS-s2. *Advances in Atmospheric Sciences*, *30*, 561–576.

Barlow, J., Berenguer, E., Carmenta, R., & França, F. (2020). Clarifying amazonia's burning crisis. *Global Change Biology*, *26*, 319–321.

Baudena, M., Dekker, S. C., van Bodegom, P. M., Cuesta, B., Higgins, S. I., Lehsten, V., Reick, C. H., Rietkerk, M., Scheiter, S., Yin, Z., Zavala, M. A., & Brovkin, V. (2015). Forests, savannas, and grasslands: Bridging the knowledge gap between ecology and Dynamic Global Vegetation Models. *Biogeosciences*, *12*, 1833–1848.

Behling, H., Berrio, J. C., & Hooghiemstra, H. (1999). Late Quaternary pollen records from the middle Caquetá river basin in central Colombian Amazon. *Palaeogeography, Palaeoclimatology, Palaeoecology*, *145*, 193–213. https://doi.org/10.1016/S0031-0182(98)00105-9

Behling, H., & da Costa, M. L. (2000). Holocene environmental changes from the Rio Curuá Record in the Caxiuanã Region, Eastern Amazon Basin. *Quaternary Research*, *53*, 369–377.

Behling, H., Keim, G., Irion, G., Junk, W., & Nunes de Mello, J. (2001). Holocene environmental changes in the Central Amazon Basin inferred from Lago Calado (Brazil). *Palaeogeography, Palaeoclimatology, Palaeoecology*, *173*, 87–101.

Bellouin, N., Collins, W. J., Culverwell, I. D., Halloran, P. R., Hardiman, S. C., Hinton, T. J., Jones, C. D., McDonald, R. E., McLaren, A. J., O'Connor, F. M., Roberts, M. J., Rodriguez, J. M., Woodward, S., Best, M. J., Brooks, M. E., Brown, A. R., Butchart, N., Dearden, C., Derbyshire, S. H., … Wiltshire, A. (2011). The HadGEM2 family of Met Office Unified Model climate configurations. *Geoscientific Model Development*, *4*, 723–757. https://doi.org/10.5194/gmd-4-723-2011

Berger, A. L. (1978). Long-Term Variations of Caloric Insolation Resulting from the Earth's Orbital Elements. *Quaternary Research*, *9*, 139–167. https://doi.org/10.1016/0033-5894(78)90064-9

Berger, A., & Loutre, M. F. (1991). Insolation values for the climate of the last 10 million years. *Quaternary Science Reviews*, *10*, 297–317.

Bernal, J. P., Cruz, F. W., Stríkis, N. M., Wang, X., Deininger, M., Catunda, M. C. A., Ortega-Obregón, C., Cheng, H., Edwards, R. L., & Auler, A. S. (2016). High-resolution Holocene South American monsoon history recorded by a speleothem from Botuverá Cave, Brazil. *Earth and Planetary Science Letters*, *450*, 186–196. https://doi.org/10.1016/j.epsl.2016.06.008

Best, M. J., Pryor, M., Clark, D. B., Rooney, G. G., Essery, R. L. H., Ménard, C. B., Edwards, J. M., Hendry, M. A., Porson, A., Gedney, N., Mercado, L. M., Sitch, S., Blyth, E., Boucher, O., Cox, P. M., Grimmond, C. S. B., & Harding, R. J. (2011). The Joint UK Land Environment Simulator (JULES), model description – Part 1: Energy and water fluxes. *Geoscientific Model Development*, *4*, 677–699. https://doi.org/10.5194/gmd-4-677-2011

Betts, R. A., Cox, P. M., Collins, M., Harris, P. P., Huntingford, C., & Jones, C. D. (2004). The role of ecosystem-atmosphere interactions in simulated Amazonian precipitation decrease and forest dieback under global climate warming. *Theoretical and Applied Climatology*, *78*, 157–175.

Boers, N., Marwan, N., Barbosa, H., & Kurths, J. (2017). A deforestation-induced tipping point for the South American monsoon system. *Scientific Reports*, *7*, 41489.

Boisier, J. P., Ciais, P., Ducharne, A., & Guimberteau, M. (2015). Projected strengthening of Amazonian dry season by constrained climate model simulations. *Nature Climate Change*, *5*, 656–660.

Braconnot, P., Harrison, S. P., Kageyama, M., Bartlein, P. J., Masson-Delmotte, V., Abe-Ouchi, A., Otto-Bliesner, B., & Zhao, Y. (2012). Evaluation of climate models using palaeoclimatic data. *Nature Climate Change*, *2*(6), 417–424. https://doi.org/10.1038/nclimate1456

Braconnot, P., Harrison, S. P., Otto-Bliesner, B., Abe-Ouchi, A., Jungclaus, J., & Peterschmitt, J. Y. (2011). The Paleoclimate Modeling Intercomparison Project contribution to CMIP5. *CLIVAR Exchanges*, *16*, 15–19.

Bradbury, J. P., Leyden, B., Salgado-Labouriau, M., Lewis, W. M., Schubert, C., Binford, M. W., Frey, D. G., Whitehead, D. R., & Weibezahn, F. H. (1981). Late quaternary environmental history of Lake Valencia, Venezuela. *Science*, *214*(4527), 1299–1305. https://doi.org/10.1126/science.214.4527.1299

Brienen, R. J. W., Phillips, O. L., Feldpausch, T. R., Gloor, E., Baker, T. R., Lloyd, J., Lopez-Gonzalez, G., Monteagudo-Mendoza, A., Malhi, Y., Lewis, S. L., Vásquez Martinez, R., Alexiades, M., Álvarez Dávila, E., Alvarez-Loayza, P., Andrade, A., Aragão, L. E. O. C., Araujo-Murakami, A., Arets, E. J. M. M., Arroyo, L., … Zagt, R. J. (2015). Long-term decline of the Amazon carbon sink. *Nature*, *519*(7543), 344–348. https://doi.org/10.1038/nature14283

Brugger, S. O., Gobet, E., van Leeuwen, J. F. N., Ledru, M.-P., Colombaroli, D., van der Knaap, W. O., Lombardo, U., Escobar-Torrez, K., Finsinger, W., Rodrigues, L., Giesche, A., Zarate, M., Veit, H., & Tinner, W. (2016). Long-term man–environment interactions in the Bolivian Amazon: 8000 years of vegetation dynamics. *Quaternary Science Reviews*, *132*, 114–128. https://doi.org/10.1016/j.quascirev.2015.11.001

Burbridge, R. E., Mayle, F. E., & Killeen, T. J. (2004). Fifty-thousand-year vegetation and climate history of Noel Kempff Mercado National Park, Bolivian Amazon. *Quaternary Research*, *61*, 215–230.

Bush, M. B., & Colinvaux, P. A. (1988). A 7000-year pollen record from the Amazon Lowlands, Ecuador. *Vegetatio*, *76*, 141–154.

Bush, M. B., Correa-Metrio, A., McMichael, C. H., Sully, S., Shadik, C. R., Valencia, B. G., Guilderson, T., Steinitz-Kannan, M., & Overpeck, J. T. (2016). A 6900-year history of landscape modification by humans in lowland Amazonia. *Quaternary Science Reviews*, *141*, 52–64. https://doi.org/10.1016/j.quascirev.2016.03.022

Bush, M. B., De Oliveira, P. E., Colinvaux, P. A., Miller, M. C., & Moreno, J. E. (2004). Amazonian paleoecological histories: one hill, three watersheds. *Palaeogeography, Palaeoclimatology, Palaeoecology*, *214*, 359–393.

Bush, M. B., Miller, M. C., De Oliveira, P. E., & Colinvaux, P. A. (2000). Two histories of environmental change and human disturbance in eastern lowland Amazonia. *The Holocene*, *10*, 543–553. https://doi.org/10.1191/095968300672647521

Bush, M. B., Silman, M. R., de Toledo, M. B., Listopad, C., Gosling, W. D., Williams, C., de Oliveira, P. E., & Krisel, C. (2007). Holocene fire and occupation in Amazonia: Records from two lake districts. *Philosophical Transactions of the Royal Society B: Biological Sciences*, *362*(1478), 209–218. https://doi.org/10.1098/rstb.2006.1980

Bush, M. B., Silman, M. R., & Listopad, C. M. C. S. (2007). A regional study of Holocene climate change and human occupation in Peruvian Amazonia. *Journal of Biogeography*, *34*, 1342–1356.

Bush, M. B., Silman, M. R., & Urrego, D. H. (2004). 48,000 years of climate and forest change in a biodiversity hot spot. *Science*, *303*, 827–829.

Bustamante, M. G., Cruz, F. W., Vuille, M., Apaéstegui, J., Strikis, N., Panizo, G., Novello, F. V., Deininger, M., Sifeddine, A., Cheng, H., Moquet, J. S., Guyot, J. L., Santos, R. V., Segura, H., & Edwards, R. L. (2016). Holocene changes in monsoon precipitation in the Andes of NE Peru based on δ18O speleothem records. *Quaternary Science Reviews*, *146*, 274–287. https://doi.org/10.1016/j.quascirev.2016.05.023

Carson, J. F., Whitney, B. S., Mayle, F. E., Iriarte, J., Prümers, H., Soto, J. D., & Watling, J. (2014). Environmental impact of geometric earthwork construction in pre-Columbian Amazonia. *Proceedings of the National Academy of Sciences*, *111*, 10497–10502. https://doi.org/10.1073/pnas.1321770111

Castanho, A. D. A., Coe, M. T., Costa, M. H., Malhi, Y., Galbraith, D. R., & Quesada, C. A. (2013). Improving simulated Amazon forest biomass and productivity by including spatial variation in biophysical parameters. *Biogeosciences*, *10*, 2255–2272. https://doi.org/10.5194/bg-10-2255-2013

Cavaleri, M. A., Coble, A. P., Ryan, M. G., Bauerle, W. L., Loescher, H. W., & Oberbauer, S. F. (2017). Tropical rainforest carbon sink declines during El Nino as a result of reduced photosynthesis and increased respiration rates. *New Phytologist*, *216*, 136–149.

Charles-Dominique, P., Blanc, P., Larpin, D., Ledru, M.-P., Riéra, B., Sarthou, C., Servant, M., & Tardy, C. (1998). Forest perturbations and biodiversity during the last ten thousand years in French Guiana. *Acta Oecologica*, *19*, 295–302. https://doi.org/10.1016/S1146-609X(98)80033-7

Cheng, H., Sinha, A., Cruz, F. W., Wang, X., Edwards, R. L., d'Horta, F. M., Ribas, C. C., Vuille, M., Stott, L. D., & Auler, A. S. (2013). Climate change patterns in Amazonia and biodiversity. *Nature Communications*, *4*, 1411. https://doi.org/10.1038/ncomms2415

Clark, D. B., Mercado, L. M., Sitch, S., Jones, C. D., Gedney, N., Best, M. J., Pryor, M., Rooney, G. G., Essery, R. L. H., Blyth, E., Boucher, O., Harding, R. J., Huntingford, C., & Cox, P. M. (2011). The Joint UK Land Environment Simulator (JULES), model description – Part 2: Carbon fluxes and vegetation dynamics. *Geoscientific Model Development*, *4*, 701–722. https://doi.org/10.5194/gmd-4-701-2011

Cohen, J. (1960). A coefficient of agreement for nominal scales. *Educational and Psychological Measurement*, *20*, 37–46. https://doi.org/10.1177/001316446002000104

Cohen, M. C. L., França, M. C., de Fátima Rossetti, D., Pessenda, L. C. R., Giannini, P. C. F., Lorente, F. L., Junior, A. Á. B., Castro, D., & Macario, K. (2014). Landscape evolution during the late Quaternary at the Doce River mouth, Espírito Santo State, Southeastern Brazil. *Palaeogeography, Palaeoclimatology, Palaeoecology*, *415*, 48–58. https://doi.org/10.1016/j.palaeo.2013.12.001

Colinvaux, P. A., De Oliveira, P. E., Moreno, J. E., Miller, M. C., & Bush, M. B. (1996). A long pollen record from lowland Amazonia: Forest and cooling in glacial times. *Science*, *274*, 85–88. https://doi.org/10.1126/science.274.5284.85

Collins, W. J., Bellouin, N., Doutriaux-Boucher, M., Gedney, N., Halloran, P., Hinton, T., Hughes, J., Jones, C. D., Joshi, M., Liddicoat, S., Martin, G., O'Connor, F., Rae, J., Senior, C., Sitch, S., Totterdell, I., Wiltshire, A., & Woodward, S. (2011). Development and evaluation of an Earth-System model - HadGEM2. *Geoscientific Model Development*, *4*, 1051–1075. https://doi.org/10.5194/gmd-4-1051-2011

Cook, B., Zeng, N., & Yoon, J.-H. (2012). Will Amazonia Dry Out? Magnitude and causes of change from IPCC climate model projections. *Earth Interactions*, *16*, 1–27. https://doi.org/10.1175/2011EI398.1

Cowling, S. A., & Shin, Y. (2006). Simulated ecosystem threshold responses to co-varying temperature, precipitation and atmospheric CO_2 within a region of Amazonia. *Global Ecology and Biogeography*, *15*, 553–566.

Cox, P. M., Betts, R. A., Collins, M., Harris, P. P., Huntingford, C., & Jones, C. D. (2004). Amazonian forest dieback under climate-carbon cycle projections for the 21st century. *Theoretical and Applied Climatology*, *78*. https://doi.org/10.1007/s00704-004-0049-4

Cox, P. M., Betts, R. A., Jones, C. D., Spall, S. A., & Totterdell, I. J. (2000). Acceleration of global warming due to carbon-cycle feedbacks in a coupled climate model. *Nature*, *408*, 184–187. https://doi.org/10.1038/35041539

Cruz, F. W., Burns, S. J., Karmann, I., Sharp, W. D., & Vuille, M. (2006). Reconstruction of regional atmospheric circulation features during the late Pleistocene in subtropical Brazil from oxygen isotope composition of speleothems. *Earth and Planetary Science Letters*, *248*, 495–507. https://doi.org/10.1016/j.epsl.2006.06.019

Cruz, F. W., Burns, S. J., Karmann, I., Sharp, W. D., Vuille, M., Cardoso, A. O., Ferrari, J. A., Silva Dias, P. L., & Viana, O. (2005). Insolation-driven changes in atmospheric circulation over the past 116,000

years in subtropical Brazil. *Nature*, *434*, 63–66. https://doi.org/10.1038/nature03365

Cruz, F. W., Vuille, M., Burns, S. J. et al (2009). Orbitally driven east-west antiphasing of South American precipitation. *Nature Geoscience*, *2*, 210–214.

Curtis, J. H., Brenner, M., & Hodell, D. A. (1999). Climate change in the Lake Valencia Basin, Venezuela, ~12600 yr BP to present. *The Holocene*, *9*, 609–619. https://doi.org/10.1191/095968399669724431

Cutler, D. R., Edwards, T. C., Beard, K. H., Cutler, A., Hess, K. T., Gibson, J., & Lawler, J. J. (2007). Random forests for classification in ecology. *Ecology*, *88*, 2783–2792. https://doi.org/10.1890/07-0539.1

Davis, M. B. (2000). Palynology after Y2K - Understanding the source area of pollen in sediments. *Annual Review of Earth and Planetary Sciences*, *28*, 1–18. https://doi.org/10.1146/annurev.earth.28.1.1

de Freitas, H. A., Pessenda, L. C. R., Aravena, R., Gouveia, S. E. M., de Souza, R. A., & Boulet, R. (2001). Late quaternary vegetation dynamics in the Southern Amazon Basin inferred from carbon isotopes in soil organic matter. *Quaternary Research*, *55*, 39–46. https://doi.org/10.1006/qres.2000.2192

Dirzo, R., & Raven, P. H. (2003). Global state of biodiversity and loss. *Annual Review of Environment and Resources*, *28*, 137–167. https://doi.org/10.1146/annurev.energy.28.050302.105532

Doughty, C. E., Metcalfe, D. B., Girardin, C. A. J., Amézquita, F. F., Cabrera, D. G., Huasco, W. H., Silva-Espejo, J. E., Araujo-Murakami, A., da Costa, M. C., Rocha, W., Feldpausch, T. R., Mendoza, A. L. M., da Costa, A. C. L., Meir, P., Phillips, O. L., & Malhi, Y. (2015). Drought impact on forest carbon dynamics and fluxes in Amazonia. *Nature*, *519*, 78–82. https://doi.org/10.1038/nature14213

Duffy, P. B., Brando, P. M., Asner, G. P., & Field, C. B. (2015). Projections of future meteorological drought and wet periods in the Amazon. *Proceedings of the National Academy of Sciences*, *112*, 13172–13177. https://doi.org/10.1073/pnas.1421010112

Eva, H. D., & Huber, O. (2005). *A proposal for defining the geographical boundaries of Amazonia: Synthesis of the results from an Expert Consultation Workshop organized by the European Commission in collaboration with the Amazon Cooperation Treaty Organization - JRC Ispra, 7–8 June 2005* (p. 1). Office for Official Publications of the European Communities, Luxembourg. https://op.europa.eu/en/publication-detail/-/publication/98b46d75-e3e7-4208-a104-465bf28e6703

Ewers, R. M., & Banks-Leite, C. (2013). Fragmentation impairs the microclimate buffering effect of tropical forests. *PLoS ONE*, *8*, e58093. https://doi.org/10.1371/journal.pone.0058093

Feldpausch, T. R., Phillips, O. L., Brienen, R. J. W., Gloor, E., Lloyd, J., Lopez-Gonzalez, G., Monteagudo-Mendoza, A., Malhi, Y., Alarcón, A., Álvarez Dávila, E., Alvarez-Loayza, P., Andrade, A., Aragao, L. E. O. C., Arroyo, L., Aymard, C. G. A., Baker, T. R., Baraloto, C., Barroso, J., Bonal, D., … Vos, V. A. (2016). Amazon forest response to repeated droughts. *Global Biogeochemical Cycles*, *30*(7), 964–982. https://doi.org/10.1002/2015gb005133

Field, C. B., Jackson, R. B., & Mooney, H. A. (1995). Stomatal responses to increased CO_2: Implications from the plant to the global scale. *Plant, Cell and Environment*, *18*(10), 1214–1225. https://doi.org/10.1111/j.1365-3040.1995.tb00630.x

Fisher, R. A., Williams, M., Lola da Costa, A., Malhi, Y., da Costa, R. F., Almeida, S., & Meir, P. (2007). The response of an Eastern Amazonian rain forest to drought stress: results and modelling analyses from a throughfall exclusion experiment. *Global Change Biology*, *13*, 2361–2378. https://doi.org/10.1111/j.1365-2486.2007.01417.x

Foley, J. A., Prentice, I. C., Ramankutty, N., Levis, S., Pollard, D., Sitch, S., & Haxeltine, A. (1996). An integrated biosphere model of land surface processes, terrestrial carbon balance, and vegetation dynamics. *Global Biogeochemical Cycles*, *10*, 603–628. https://doi.org/10.1029/96GB02692

Fontes, D., Cordeiro, R. C., Martins, G. S., Behling, H., Turcq, B., Sifeddine, A., Seoane, J., Moreira, L. S., & Rodrigues, R. A. (2017). Paleoenvironmental dynamics in South Amazonia, Brazil, during the last 35,000 years inferred from pollen and geochemical records of Lago do Saci. *Quaternary Science Reviews*, *173*, 161–180. https://doi.org/10.1016/j.quascirev.2017.08.021

Galbraith, D. R., Levy, P. E., Sitch, S., Huntingford, C., Cox, P. M., Williams, M., & Meir, P. (2010). Multiple mechanisms of Amazonian forest biomass losses in three dynamic global vegetation models under climate change. *New Phytologist*, *187*, 647–665. https://doi.org/10.1111/j.1469-8137.2010.03350.x

Gash, J. H. C., Huntingford, C., Marengo, J. A., Betts, R. A., Cox, P. M., Fisch, G., Fu, R., Gandu, A. W., Harris, P. P., Machado, L. A. T., von Randow, C., & Silva Dias, M. A. (2004). Amazonian climate: Results and future research. *Theoretical and Applied Climatology*, *78*, 1–7. https://doi.org/10.1007/s00704-004-0052-9

Gatti, L. V., Gloor, M., Miller, J. B., Doughty, C. E., Malhi, Y., Domingues, L. G., Basso, L. S., Martinewski, A., Correia, C. S. C., Borges, V. F., Freitas, S., Braz, R., Anderson, L. O., Rocha, H., Grace, J., Phillips, O. L., & Lloyd, J. (2014). Drought sensitivity of Amazonian carbon balance revealed by atmospheric measurements. *Nature*, *506*, 76–80. https://doi.org/10.1038/nature12957

Gond, V., Freycon, V., Molino, J.-F., Brunaux, O., Ingrassia, F., Joubert, P., Pekel, J.-F., Prévost, M.-F., Thierron, V., Trombe, P.-J., & Sabatier, D. (2011). Broad-scale spatial pattern of forest landscape types in the Guiana Shield. *International Journal of Applied Earth Observations and Geoinformation*, *13*, 357–367. https://doi.org/10.1016/j.jag.2011.01.004

Good, P., Jones, C., Lowe, J., Betts, R., Booth, B., & Huntingford, C. (2011). Quantifying environmental drivers of future tropical forest extent. *Journal of Climate*, *24*, 1337–1349.

Good, P., Jones, C., Lowe, J., Betts, R. A., & Gedney, N. (2013). Comparing tropical forest projections from two generations of hadley centre earth system models, HadGEM2-ES and HadCM3LC. *Journal of Climate*, *26*, 495–511. https://doi.org/10.1175/JCLI-D-11-00366.1

Gordon, H. B., O'Farrell, S. P., Collier, M. A., Dix, M., Rotstayn, L., Kowalczyk, E., Hirst, T., & Watterson, I. (2010). The CSIRO Mk3.5 climate model. The Centre for Australian Weather and Climate Research Technical Report No. 21, Aspendale, Victoria, Australia.

Gordon, H. B., Rotstayn, L. D., McGregor, J. L., Dix, M. R., Kowalczyk, E. A., O'Farrell, S. P., Waterman, L. J., Wilson, S. G., Collier, M. A., Watterson, I. G., & Elliott, T. I. (2002). The CSIRO Mk3 climate system model. CSIRO Atmospheric Research Technical Paper No. 60, Aspendale, Victoria, Australia.

Gouveia, S. E. M., Pessenda, L. C. R., Aravena, R. et al (2002). Carbon isotopes in charcoal and soils in studies of paleovegetation and climate changes during the late Pleistocene and the Holocene in the southeast and centerwest regions of Brazil. *Global and Planetary Change*, *33*, 95–106.

Guimarães, J. T. F., Cohen, M. C. L., França, M. C., Alves, I. C. C., Smith, C. B., Pessenda, L. C. R., & Behling, H. (2013). An integrated approach to relate Holocene climatic, hydrological, morphological and vegetation changes in the southeastern Amazon region. *Vegetation History and Archaeobotany*, *22*, 185–198.

Harper, A. B., Baker, I. T., Denning, A. S., Randall, D. A., Dazlich, D., & Branson, M. (2014). Impact of evapotranspiration on dry season climate in the Amazon forest. *Journal of Climate*, *27*, 574–591.

Harris, I. C., & Jones, P. D. (2017). University of East Anglia Climatic Research Unit. CRU TS4.01: Climatic Research Unit (CRU) Time-Series (TS) version 4.01 of high-resolution gridded data of month-by-month variation in climate (Jan. 1901- Dec. 2016). Centre for Environmental Data Analysis.

Harris, I. C., Jones, P. D., Osborn, T. J., & Lister, D. H. (2014). Updated high-resolution grids of monthly climatic observations - the CRU TS3.10 Dataset. *International Journal of Climatology*, *34*, 623–642. https://doi.org/10.1002/joc.3711

Harrison, S. P., Bartlein, P. J., Izumi, K., Li, G., Annan, J., Hargreaves, J., Braconnot, P., & Kageyama, M. (2015). Evaluation of CMIP5 palaeo-simulations to improve climate projections. *Nature Climate Change*, *5*, 735–743. https://doi.org/10.1038/nclimate2649

Harrison, S. P., Braconnot, P., Joussaume, S., Hewitt, C., & Stouffer, R. J. (2002). Fourth International Workshop of the Palaeoclimate Modelling Intercomparison Project (PMIP): Launching PMIP2 Phase II. *EOS*, *83*, 447.

Haug, G. H., Hughen, K. A., Sigman, D. M., Peterson, L. C., & Röhl, U. (2001). Southward migration of the intertropical convergence zone through the Holocene. *Science*, *293*, 1304–1308. https://doi.org/10.1126/science.1059725

Haywood, A. M., Valdes, P. J., Aze, T., Barlow, N., Burke, A., Dolan, A. M., von der Heydt, A. S., Hill, D. J., Jamieson, S. S. R., Otto-Bliesner, B. L., Salzmann, U., Saupe, E., & Voss, J. (2019). What can Palaeoclimate Modelling do for you? *Earth Systems and Environment*, *3*(1), 1–18. https://doi.org/10.1007/s41748-019-00093-1

Hermanowski, B., da Costa, M. L., & Behling, H. (2012). Environmental changes in southeastern Amazonia during the last 25,000yr revealed from a paleoecological record. *Quaternary Research*, *77*, 138–148.

Hermanowski, B., da Costa, M. L., & Behling, H. (2014). Possible linkages of palaeofires in southeast Amazonia to a changing climate since the Last Glacial Maximum. *Vegetation History and Archaeobotany*, 1–14.

Hermanowski, B., da Costa, M. L., Carvalho, A. T., & Behling, H. (2012). Palaeoenvironmental dynamics and underlying climatic changes in southeast Amazonia (Serra Sul dos Carajás, Brazil) during the late Pleistocene and Holocene. *Palaeogeography, Palaeoclimatology, Palaeoecology*, *365–366*, 227–246.

Horbe, A. M. C., Behling, H., Nogueira, A. C. R., & Mapes, R. (2011). Environmental changes in the western Amazônia: Morphological framework, geochemistry, palynology and radiocarbon dating data. *Anais da Academia Brasileira de Ciências*, *83*, 863–874. https://doi.org/10.1590/S0001-37652011005000030

Huntingford, C., Fisher, R. A., Mercado, L., Booth, B. B. B., Sitch, S., Harris, P. P., Cox, P. M., Jones, C. D., Betts, R. A., Malhi, Y., Harris, G. R., Collins, M., & Moorcroft, P. (2008). Towards quantifying uncertainty in predictions of Amazon "dieback". *Philosophical Transactions of the Royal Society B: Biological Sciences*, *363*, 1857–1864. https://doi.org/10.1098/rstb.2007.0028

Huntingford, C., Zelazowski, P., Galbraith, D., Mercado, L. M., Sitch, S., Fisher, R., Lomas, M., Walker, A. P., Jones, C. D., Booth, B. B. B., Malhi, Y., Hemming, D., Kay, G., Good, P., Lewis, S. L., Phillips, O. L., Atkin, O. K., Lloyd, J., Gloor, E., … Cox, P. M. (2013). Simulated resilience of tropical rainforests to CO_2-induced climate change. *Nature Geoscience*, *6*, 268–273. https://doi.org/10.1038/ngeo1741

Irion, G., Bush, M. B., Nunes de Mello, J. A., Stüben, D., Neumann, T., Müller, G., Morais de, J. O., & Junk, J. W. (2006). A multiproxy palaeoecological record of Holocene lake sediments from the Rio Tapajós, eastern Amazonia. *Palaeogeography, Palaeoclimatology, Palaeoecology*, *240*, 523–535. https://doi.org/10.1016/j.palaeo.2006.03.005

Jeffrey, S., Rotstayn, L., Collier, M., Dravitzki, S., Hamalainen, C., Moeseneder, C., Wong, K., & Skytus, J. (2013). Australia's CMIP5 submission using the CSIRO Mk3.6 model. *Australian Meteorological and Oceanographic Journal*, *63*, 1–13. https://doi.org/10.22499/2.6301.001

Joetzjer, E., Douville, H., Delire, C., & Ciais, P. (2013). Present-day and future Amazonian precipitation in global climate models: CMIP5 versus CMIP3. *Climate Dynamics*, *41*, 2921–2936. https://doi.org/10.1007/s00382-012-1644-1

Joussaume, S., & Taylor, K. E. (1995). Status of the paleoclimate modeling intercomparison project (PMIP). In: *Proceedings of the First International AMIP Scientific Conference*, *WCRP-92 Report* (pp. 425–430).

Kageyama, M., Braconnot, P., Bopp, L., Caubel, A., Foujols, M.-A., Guilyardi, E., Khodri, M., Lloyd, J., Lombard, F., Mariotti, V., Marti, O., Roy, T., & Woillez, M.-N. (2013). Mid-Holocene and last glacial maximum climate simulations with the IPSL model—part I: Comparing IPSL_CM5A to IPSL_CM4. *Climate Dynamics*, *40*(9-10), 2447–2468. https://doi.org/10.1007/s00382-012-1488-8

Kageyama, M., Braconnot, P., Bopp, L., Mariotti, V., Roy, T., Woillez, M.-N., Caubel, A., Foujols, M.-A., Guilyardi, E., Khodri, M., Lloyd, J., Lombard, F., & Marti, O. (2013). Mid-Holocene and last glacial maximum climate simulations with the IPSL model: Part II: Modeldata comparisons. *Climate Dynamics*, *40*(9–10), 2469–2495. https://doi.org/10.1007/s00382-012-1499-5

Kanner, L. C., Burns, S. J., Cheng, H., Edwards, R. L., & Vuille, M. (2013). High-resolution variability of the South American summer monsoon over the last seven millennia: Insights from a speleothem record from the central Peruvian Andes. *Quaternary Science Reviews*, *75*, 1–10.

Kucharik, C. J., Foley, J. A., Delire, C., Fisher, V. A., Coe, M. T., Lenters, J. D., Young-Molling, C., Ramankutty, N., Norman, J. M., & Gower, S. T. (2000). Testing the performance of a dynamic global ecosystem model: Water balance, carbon balance, and vegetation structure. *Global Biogeochemical Cycles*, *14*(3), 795–825. https://doi.org/10.1029/1999gb001138

Langan, L., Higgins, S. I., & Scheiter, S. (2017). Climate-biomes, pedo-biomes or pyro-biomes: which world view explains the tropical forest-savanna boundary in South America? *Journal of Biogeography*, *44*, 2319–2330.

Langenbrunner, B., Pritchard, M. S., Kooperman, G. J., & Randerson, J. T. (2019). Why does Amazon precipitation decrease when tropical forests respond to increasing CO_2? *Earth's Future*, *7*, 450–468. https://doi.org/10.1029/2018EF001026

Lapola, D. M., Oyama, M. D., & Nobre, C. A. (2009). Exploring the range of climate biome projections for tropical South America: The role of CO_2 fertilization and seasonality. *Biogeosciences*, *23*, n/a–n/a.

Ledru, M.-P. (2001). Late Holocene rainforest disturbance in French Guiana. *Review of Palaeobotany and Palynology*, *115*, 161–176. https://doi.org/10.1016/S0034-6667(01)00068-9

Ledru, M.-P., Ceccantini, G., Gouveia, S. E. M., López-Sáez, J. A., Pessenda, L. C. R., & Ribeiro, A. S. (2006). Millenial-scale climatic and vegetation changes in a northern Cerrado (Northeast, Brazil) since the Last Glacial Maximum. *Quaternary Science Reviews*, *25*, 1110–1126. https://doi.org/10.1016/j.quascirev.2005.10.005

Levine, N. M., Zhang, K. E., Longo, M., Baccini, A., Phillips, O. L., Lewis, S. L., Alvarez-Dávila, E., Segalin de Andrade, A. C., Brienen, R. J. W., Erwin, T. L., Feldpausch, T. R., Monteagudo Mendoza, A. L., Nuñez Vargas, P., Prieto, A., Silva-Espejo, J. E., Malhi, Y., & Moorcroft, P. R. (2016). Ecosystem heterogeneity determines the ecological resilience of the Amazon to climate change. *Proceedings of the National Academy of Sciences of the United States of America*, *113*, 793–797. https://doi.org/10.1073/pnas.1511344112

Liu, K.-B., & Colinvaux, P. A. (1988). A 5200-year history of Amazon rain forest. *Journal of Biogeography*, *15*, 231. https://doi.org/10.2307/2845412

Lloyd, J., & Farquhar, G. D. (2008). Effects of rising temperatures and [CO2] on the physiology of tropical forest trees. *Philosophical Transactions of the Royal Society B: Biological Sciences*, *363*, 1811–1817.

Maezumi, S. Y., Power, M. J., Mayle, F. E., McLauchlan, K. K., & Iriarte, J. (2015). Effects of past climate variability on fire and vegetation in the cerrãdo savanna of the Huanchaca Mesetta, NE Bolivia. *Climate of the Past*, *11*, 835–853. https://doi.org/10.5194/cp-11-835-2015

Malhi, Y., Aragao, L. E. O. C., Galbraith, D., Huntingford, C., Fisher, R., Zelazowski, P., Sitch, S., McSweeney, C., & Meir, P. (2009). Exploring the likelihood and mechanism of a climate-change-induced dieback of the Amazon rainforest. *Proceedings of the National Academy*

of Sciences, *106*(49), 20610–20615. https://doi.org/10.1073/pnas.0804619106

Malhi, Y., Phillips, O. L., Lloyd, J., Baker, T., Wright, J., Almeida, S., Arroyo, L., Frederiksen, T., Grace, J., Higuchi, N., Killeen, T., Laurance, W. F., Leaño, C., Lewis, S., Meir, P., Monteagudo, A., Neill, D., Núñez Vargas, P., Panfil, S. N., … Vinceti, B. (2002). An international network to monitor the structure, composition and dynamics of Amazonian forests (RAINFOR). *Journal of Vegetation Science*, *13*(3), 439–450. https://doi.org/10.1111/j.1654-1103.2002.tb02068.x

Malhi, Y., Roberts, J. T., Betts, R. A., Killeen, T. J., Li, W., & Nobre, C. A. (2008). Climate change, deforestation, and the fate of the Amazon. *Science*, *319*, 169–172.

Malhi, Y., & Wright, J. (2004). Spatial patterns and recent trends in the climate of tropical rainforest regions. *Philosophical Transactions of the Royal Society B: Biological Sciences*, *359*, 311–329. https://doi.org/10.1098/rstb.2003.1433

Marchant, R., Cleef, A., Harrison, S. P., Hooghiemstra, H., Markgraf, V., van Boxel, J., Ager, T., Almeida, L., Anderson, R., Baied, C., Behling, H., Berrio, J. C., Burbridge, R., Björck, S., Byrne, R., Bush, M., Duivenvoorden, J., Flenley, J., De Oliveira, P., … Wille, M. (2009). Pollen-based biome reconstructions for Latin America at 0, 6000 and 18 000 radiocarbon years ago. *Climate of the Past*, *5*, 725–767. https://doi.org/10.5194/cp-5-725-2009

Marcott, S. A., Shakun, J. D., Clark, P. U., & Mix, A. C. (2013). A reconstruction of regional and global temperature for the past 11,300 years. *Science*, *399*, 1198–1201.

Marthews, T. R., Quesada, C. A., Galbraith, D. R., Malhi, Y., Mullins, C. E., Hodnett, M. G., & Dharssi, I. (2014). High-resolution hydraulic parameter maps for surface soils in tropical South America. *Geoscientific Model Development*, *7*, 711–723. https://doi.org/10.5194/gmd-7-711-2014

Marti, O., Braconnot, P., Dufresne, J.-L., Bellier, J., Benshila, R., Bony, S., Brockmann, P., Cadule, P., Caubel, A., Codron, F., de Noblet, N., Denvil, S., Fairhead, L., Fichefet, T., Foujols, M.-A., Friedlingstein, P., Goosse, H., Grandpeix, J.-Y., Guilyardi, E., … Talandier, C. (2010). Key features of the IPSL ocean atmosphere model and its sensitivity to atmospheric resolution. *Climate Dynamics*, *34*, 1–26. https://doi.org/10.1007/s00382-009-0640-6

May, P. H., Soares-Filho, B. S., & Strand, J. (2013). *How much is the Amazon Worth? The state of knowledge concerning the value of preserving Amazon rainforests*. The World Bank.

Mayle, F. E., Burbridge, R. E., & Killeen, T. J. (2000). Millennial-scale dynamics of southern Amazonian rain forests. *Science*, *290*, 2291–2294. https://doi.org/10.1126/science.290.5500.2291

McMichael, C. N. H., Bush, M. B., Piperno, D. R., Silman, M. R., Zimmerman, A. R., & Anderson, C. (2012). Spatial and temporal scales of pre-Columbian disturbance associated with western Amazonian lakes. *The Holocene*, *22*, 131–141.

Meinshausen, M., Smith, S. J., Calvin, K., Daniel, J. S., Kainuma, M. L. T., Lamarque, J.-F., Matsumoto, K., Montzka, S. A., Raper, S. C. B., Riahi, K., Thomson, A., Velders, G. J. M., & van Vuuren, D. P. P. (2011). The RCP greenhouse gas concentrations and their extensions from 1765 to 2300. *Climatic Change*, *109*(1–2), 213–241. https://doi.org/10.1007/s10584-011-0156-z

Meir, P., & Woodward, F. I. (2010). Amazonian rain forests and drought: Response and vulnerability. *New Phytologist*, *187*, 553–557.

Montoya, E., & Rull, V. (2011). Gran Sabana fires (SE Venezuela): A paleoecological perspective. *Quaternary Science Reviews*, *30*, 3430–3444. https://doi.org/10.1016/j.quascirev.2011.09.005

Montoya, E., Rull, V., & Nogué, S. (2011). Early human occupation and land use changes near the boundary of the Orinoco and the Amazon basins (SE Venezuela): Palynological evidence from El Paují record. *Palaeogeography, Palaeoclimatology, Palaeoecology*, *310*, 413–426.

Montoya, E., Rull, V., Stansell, N. D., Abbott, M. B., Nogué, S., Bird, B. W., & Díaz, W. A. (2011). Forest–savanna–morichal dynamics in relation to fire and human occupation in the southern Gran Sabana (SE Venezuela) during the last millennia. *Quaternary Research*, *76*, 335–344.

Murphy, B. P., & Bowman, D. M. J. S. (2012). What controls the distribution of tropical forest and savanna? *Ecology Letters*, *15*, 748–758.

Nobre, C. A., Sampaio, G., Borma, L. S., Castilla-Rubio, J. C., Silva, J. S., & Cardoso, M. (2016). Land-use and climate change risks in the Amazon and the need of a novel sustainable development paradigm. *Proceedings of the National Academy of Sciences of the United States of America*, *113*(39), 10759–10768.

Olson, D. M., Dinerstein, E., Wikramanayake, E. D., Burgess, N. D., Powell, G. V. N., Underwood, E. C., D'amico, J. A., Itoua, I., Strand, H. E., Morrison, J. C., Loucks, C. J., Allnutt, T. F., Ricketts, T. H., Kura, Y., Lamoreux, J. F., Wettengel, W. W., Hedao, P., & Kassem, K. R. (2001). Terrestrial ecoregions of the world: A new map of life on earth. A new global map of terrestrial ecoregions provides an innovative tool for conserving biodiversity. *BioScience*, *51*, 933–938.

Pan, Y., Birdsey, R. A., Fang, J., Houghton, R., Kauppi, P. E., Kurz, W. A., Phillips, O. L., Shvidenko, A., Lewis, S. L., Canadell, J. G., Ciais, P., Jackson, R. B., Pacala, S. W., McGuire, A. D., Piao, S., Rautiainen, A., Sitch, S., & Hayes, D. (2011). A large and persistent carbon sink in the world's forests. *Science*, *333*, 988–993. https://doi.org/10.1126/science.1201609

Pessenda, L. C. R., Boulet, R., Aravena, R., Rosolen, V., Gouveia, S. E. M., Ribeiro, A. S., & Lamotte, M. (2001). Origin and dynamics of soil organic matter and vegetation changes during the Holocene in a forest-savanna transition zone, Brazilian Amazon region. *The Holocene*, *11*, 250–254.

Pessenda, L. C. R., Gomes, B. M., Aravena, R., Ribeiro, A. S., Boulet, R., & Gouveia, S. E. M. (1998). The carbon isotope record in soils along a forest-cerrado ecosystem transect: implications for vegetation changes in the Rondonia state, southwestern Brazilian Amazon region. *The Holocene*, *8*, 599–603.

Pessenda, L. C. R., Ledru, M.-P., Gouveia, S. E. M., Aravena, R., Ribeiro, A. S., Bendassolli, J. A., & Boulet, R. (2005). Holocene palaeoenvironmental reconstruction in northeastern Brazil inferred from pollen, charcoal and carbon isotope records. *The Holocene*, *15*, 812–820.

Pessenda, L. C. R., Ribeiro, A. D. S., Gouveia, S. E. M., Aravena, R., Boulet, R., & Bendassolli, J. A. (2004). Vegetation dynamics during the late Pleistocene in the Barreirinhas region, Maranhão State, northeastern Brazil, based on carbon isotopes in soil organic matter. *Quaternary Research*, *62*, 183–193. https://doi.org/10.1016/j.yqres.2004.06.003

Phillips, O. L., Aragão, L. E. O. C., Lewis, S. L., Fisher, J. B., Lloyd, J., López-González, G., Malhi, Y., Monteagudo, A., Peacock, J., Quesada, C. A., van der Heijden, G., Almeida, S., Amaral, I., Arroyo, L., Aymard, G., Baker, T. R., Bánki, O., Blanc, L., Bonal, D., … Torres-Lezama, A. (2009). Drought sensitivity of the Amazon rainforest. *Science*, *323*(5919), 1344–1347. https://doi.org/10.1126/science.1164033

Potapov, P., Hansen, M. C., Laestadius, L., Turubanova, S., Yaroshenko, A., Thies, C., Smith, W., Zhuravleva, I., Komarova, A., Minnemeyer, S., & Esipova, E. (2017). The last frontiers of wilderness: Tracking loss of intact forest landscapes from 2000 to 2013. *Science Advances*, *3*(1), https://doi.org/10.1126/sciadv.1600821

Prado, L. F., Wainer, I., Chiessi, C. M., Ledru, M.-P., & Turcq, B. (2013). A mid-Holocene climate reconstruction for eastern South America. *Climate of the Past*, *9*, 2117–2133. https://doi.org/10.5194/cp-9-2117-2013

Raia, A., & Cavalcanti, I. F. A. (2008). The life cycle of the South American monsoon system. *Journal of Climate*, *21*, 6227–6246. https://doi.org/10.1175/2008JCLI2249.1

Rammig, A., Jupp, T., Thonicke, K., Tietjen, B., Heinke, J., Ostberg, S., Lucht, W., Cramer, W., & Cox, P. (2010). Estimating the risk of Amazonian forest dieback. *New Phytologist*, *187*, 694–706. https://doi.org/10.1111/j.1469-8137.2010.03318.x

Rein, B., Lückge, A., Reinhardt, L., Sirocko, F., Wolf, A., & Dullo, W.-C. (2005). El Niño variability off Peru during the last 20,000 years.

Paleoceanography, *20*, 1–17. https://doi.org/10.1029/2004PA001099

Rowe, H. D., Dunbar, R. B., Mucciarone, D. A., Seltzer, G. O., Baker, P. A., & Fritz, S. C. (2002). Insolation, moisture balance and climate change on the South American Altiplano since the last glacial maximum. *Climatic Change*, *52*, 175–199.

Rull, V. (2004). An evaluation of the Lost World and Vertical Displacement hypotheses in the Chimanta Massif, Venezuelan Guayana. *Global Ecology and Biogeography Letters*, *13*, 141–148.

Rull, V. (2005). Palaeovegetational and palaeoenvironmental trends in the summit of the Guaiquinima massif (Venezuelan Guayana) during the Holocene. *Journal of Quaternary Science*, *20*, 135–145. https://doi.org/10.1002/jqs.896

Rull, V., Montoya, E., Vegas-Vilarrúbia, T., & Ballesteros, T. (2015). New insights on palaeofires and savannisation in northern South America. *Quaternary Science Reviews*, *122*, 158–165.

Schaphoff, S., Lucht, W., Gerten, D., Sitch, S., Cramer, W., & Prentice, I. C. (2006). Terrestrial biosphere carbon storage under alternative climate projections. *Climatic Change*, *74*, 97–122. https://doi.org/10.1007/s10584-005-9002-5

Schmidt, G. A. (2010). Enhancing the relevance of palaeoclimate model/data comparisons for assessments of future climate change. *Journal of Quaternary Science*, *25*(1), 79–87. https://doi.org/10.1002/jqs.1314

Schmidt, G. A., Annan, J. D., Bartlein, P. J., Cook, B. I., Guilyardi, E., Hargreaves, J. C., Harrison, S. P., Kageyama, M., LeGrande, A. N., Konecky, B., Lovejoy, S., Mann, M. E., Masson-Delmotte, V., Risi, C., Thompson, D., Timmermann, A., Tremblay, L.-B., & Yiou, P. (2014). Using palaeo-climate comparisons to constrain future projections in CMIP5. *Climate of the Past*, *10*, 221–250. https://doi.org/10.5194/cp-10-221-2014

Schmidt, G. A., Kelley, M., Nazarenko, L., Ruedy, R., Russell, G. L., Aleinov, I., Bauer, M., Bauer, S. E., Bhat, M. K., Bleck, R., Canuto, V., Chen, Y.-H., Cheng, Y. E., Clune, T. L., Del Genio, A., de Fainchtein, R., Faluvegi, G., Hansen, J. E., Healy, R. J., … Zhang, J. (2014). Configuration and assessment of the GISS ModelE2 contributions to the CMIP5 archive. *Journal of Advances in Modeling Earth Systems*, *6*, 141–184. https://doi.org/10.1002/2013MS000265

Seltzer, G. O., Rodbell, D., & Burns, S. J. (2000). Isotopic evidence for late Quaternary climatic change in tropical South America. *Geology*, *28*, 35–38. https://doi.org/10.1130/0091-7613(2000)28<35:IEFLQC>2.0.CO;2

Shukla, J., Nobre, C., & Sellers, P. (1990). Amazon deforestation and climate change. *Science*, *247*, 1322–1325.

Sifeddine, A., Albuquerque, A. L. S., & Ledru, M.-P. (2003). A 21 000 cal years paleoclimatic record from Caçó Lake, northern Brazil: Evidence from sedimentary and pollen analyses. *Palaeogeography, Palaeoclimatology, Palaeoecology*, *189*, 25–34.

Sifeddine, A., Bertrand, P., & Fournier, M. (1994). La sédimentation organique lacustre en milieu tropical humide (Carajás, Amazonie orientale, Brésil): Relation avec les changements climatiques au cours des 60,000 dernières années. *Bulletin de la Societe Geologique de France*, *165*, 613–621.

Sifeddine, A., Martin, L., Turcq, B., Volkmer-Ribeiro, C., Soubiès, F., Cordeiro, R. C., & Suguio, K. (2001). Variations of the Amazonian rainforest environment: a sedimentological record covering 30,000 years. *Palaeogeography, Palaeoclimatology, Palaeoecology*, *168*, 221–235. https://doi.org/10.1016/S0031-0182(00)00256-X

Silva, V. B. S., & Kousky, V. E. (2012). The South American monsoon system: Climatology and variability. In S.-Y. Wang (Ed.), *Modern climatology* (pp. 123–152). InTech. http://www.intechopen.com/books/modern-climatology/the-south-american-monsoon-system-climateology-and-variability

Singarayer, J. S., Valdes, P. J., & Roberts, W. H. G. (2017). Ocean dominated expansion and contraction of the late Quaternary tropical rainbelt. *Scientific Reports*, *7*.

Sitch, S., Huntingford, C., Gedney, N., Levy, P. E., Lomas, M., Piao, S. L., Betts, R., Ciais, P., Cox, P., Friedlingstein, P., Jones, C. D., Prentice, I. C., & Woodward, F. I. (2008). Evaluation of the terrestrial carbon cycle, future plant geography and climate-carbon cycle feedbacks using five Dynamic Global Vegetation Models (DGVMs). *Global Change Biology*, *14*(9), 2015–2039. https://doi.org/10.1111/j.1365-2486.2008.01626.x

Skole, D., & Tucker, C. (1993). Tropical deforestation and habitat fragmentation in the Amazon - satellite data from 1978 to 1988. *Science*, *260*, 1905–1910.

Smith, R. J., & Mayle, F. E. (2018). Impact of mid- to late Holocene precipitation changes on vegetation across lowland tropical South America: A paleo-data synthesis. *Quaternary Research*, *89*, 134–155.

Smith, R. J., Mayle, F. E., Maezumi, S. Y., & Power, M. J. (2021). Relating pollen representation to an evolving Amazonian landscape between the last glacial maximum and late Holocene. *Quaternary Research*, *99*, 63–79. https://doi.org/10.1017/qua.2020.64

Soares-Filho, B. S., Nepstad, D. C., Curran, L. M., Cerqueira, G. C., Garcia, R. A., Ramos, C. A., Voll, E., McDonald, A., Lefebvre, P., & Schlesinger, P. (2006). Modelling conservation in the Amazon basin. *Nature*, *440*, 520–523. https://doi.org/10.1038/nature04389

Strikis, N. M., Cruz, F. W., Cheng, H., Karmann, I., Edwards, R. L., Vuille, M., Wang, X., de Paula, M. S., Novello, V. F., & Auler, A. S. (2011). Abrupt variations in South American monsoon rainfall during the Holocene based on a speleothem record from central-eastern Brazil. *Geology*, *39*, 1075–1078. https://doi.org/10.1130/G32098.1

Sueyoshi, T., Ohgaito, R., Yamamoto, A., Chikamoto, M. O., Hajima, T., Okajima, H., Yoshimori, M., Abe, M., O'ishi, R., Saito, F., Watanabe, S., Kawamiya, M., & Abe-Ouchi, A. (2013). Set-up of the PMIP3 paleoclimate experiments conducted using an Earth system model, MIROC-ESM. *Geoscientific Model Development*, *6*, 819–836. https://doi.org/10.5194/gmd-6-819-2013

Sugita, S. (1994). Pollen representation of vegetation in quaternary sediments–Theory and method in patchy vegetation. *Journal of Ecology*, *82*, 881–897. https://doi.org/10.2307/2261452

Sugita, S. (2007). Theory of quantitative reconstruction of vegetation I: Pollen from large sites REVEALS regional vegetation composition. *The Holocene*, *17*, 229–241. https://doi.org/10.1177/0959683607075837

Sugita, S., Gaillard, M. J., & Broström, A. (1999). Landscape openness and pollen records: A simulation approach. *The Holocene*, *9*, 409–421. https://doi.org/10.1191/095968399666429937

Swann, A. L. S., Hoffman, F. M., Koven, C. D., & Randerson, J. T. (2016). Plant responses to increasing CO_2 reduce estimates of climate impacts on drought severity. *Proceedings of the National Academy of Sciences of the United States of America*, *113*, 10019–10024.

Taylor, K. E., Stouffer, R. J., & Meehl, G. A. (2012). An overview of CMIP5 and the experiment design. *Bulletin of the American Meteorological Society*, *93*, 485–498.

Thompson, L. G., Davis, M., Mosley-Thompson, E., Sowers, T. A., Henderson, K. A., Zagorodnov, V. S., Lin, P.-N., Mikhalenko, N., Campen, R. K., Bolzan, J. F., Cole-Dai, J., & Francou, B. (1998). A 25,000-year tropical climate history from Bolivian ice cores. *Science*, *282*, 1858–1864. https://doi.org/10.1126/science.282.5395.1858

Urrego, D. H., Bush, M. B., Silman, M. R., Niccum, B. A., De La Rosa, P., McMichael, C. H., Hagen, S., & Palace, M. (2013). Holocene fires, forest stability and human occupation in south-western Amazonia. *Journal of Biogeography*, *40*(3), 521–533. https://doi.org/10.1111/jbi.12016

van Breukelen, M. R., Vonhof, H. B., Hellstrom, J. C., Wester, W. C. G., & Kroon, D. (2008). Fossil dripwater in stalagmites reveals Holocene temperature and rainfall variation in Amazonia. *Earth and Planetary Science Letters*, *275*, 54–60.

Voldoire, A., Sanchez-Gomez, E., & Mélia, D. Y. (2013). The CNRM-CM5.1 global climate model: description and basic evaluation. *Climate Dynamics*, *40*, 2091–2121.

Wang, X., Auler, A. S., Edwards, R. L., Cheng, H., Ito, E., Wang, Y., Kong, X., & Solheid, M. (2007). Millennial-scale precipitation changes in southern Brazil over the past 90,000 years. *Geophysical Research Letters*, *34*(23). https://doi.org/10.1029/2007gl031149

Wang, X., Edwards, R. L., Auler, A. S., Cheng, H., Kong, X., Wang, Y., Cruz, F. W., Dorale, J. A., & Chiang, H.-W. (2017). Hydroclimate changes across the Amazon lowlands over the past 45,000 years. *Nature*, *541*, 204–207. https://doi.org/10.1038/nature20787

Watanabe, S., Hajima, T., Sudo, K., Nagashima, T., Takemura, T., Okajima, H., Nozawa, T., Kawase, H., Abe, M., Yokohata, T., Ise, T., Sato, H., Kato, E., Takata, K., Emori, S., & Kawamiya, M. (2011). MIROC-ESM 2010: Model description and basic results of CMIP5-20c3m experiments. *Geoscientific Model Development*, *4*(4), 845–872. https://doi.org/10.5194/gmd-4-845-2011

Watling, J., Iriarte, J., Mayle, F. E. et al (2017). Impact of pre-Columbian "geoglyph" builders on Amazonian forests. *Proceedings of the National Academy of Sciences of the United States of America*, *114*, 1868–1873.

Weedon, G. P., Balsamo, G., Bellouin, N., Gomes, S., Best, M. J., & Viterbo, P. (2014). The WFDEI meteorological forcing data set: WATCH Forcing Data methodology applied to ERA-Interim reanalysis data. *Water Resources Research*, *50*, 7505–7514.

Weng, C., Bush, M. B., & Athens, J. S. (2002). Holocene climate change and hydrarch succession in lowland Amazonian Ecuador. *Review of Palaeobotany and Palynology*, *120*, 73–90.

Werth, D., & Avissar, R. (2002). The local and global effects of Amazon deforestation. *Journal of Geophysical Research*, *107*, LBA 55–1–LBA 55–8. https://doi.org/10.1029/2001JD000717

Whitney, B. S., & Mayle, F. E. (2012). Pediastrum species as potential indicators of lake-level change in tropical South America. *Journal of Paleolimnology*, *47*, 601–615. https://doi.org/10.1007/s10933-012-9583-8

Whitney, B. S., Mayle, F. E., Punyasena, S. W., Fitzpatrick, K. A., Burn, M. J., Guillen, R., Chavez, E., Mann, D., Pennington, R. T., & Metcalfe, S. E. (2011). A 45kyr palaeoclimate record from the lowland interior of tropical South America. *Palaeogeography, Palaeoclimatology, Palaeoecology*, *307*, 177–192. https://doi.org/10.1016/j.palaeo.2011.05.012

Woodward, F. I., & Lomas, M. R. (2004). Vegetation dynamics–simulating responses to climatic change. *Biological Reviews of the Cambridge Philosophical Society*, *79*, 643–670. https://doi.org/10.1017/S1464793103006419

Woodward, F. I., Smith, T. M., & Emanuel, W. R. (1995). A global land primary productivity and phytogeography model. *Global Biogeochemical Cycles*, *9*, 471–490. https://doi.org/10.1029/95GB02432

Zech, M., Zech, R., Morrás, H., Moretti, L., Glaser, B., & Zech, W. (2009). Late Quaternary environmental changes in Misiones, subtropical NE Argentina, deduced from multi-proxy geochemical analyses in a palaeosol-sediment sequence. *Quaternary International*, *196*, 121–136. https://doi.org/10.1016/j.quaint.2008.06.006

Zhang, K., de Almeida Castanho, A. D., Galbraith, D. R., Moghim, S., Levine, N. M., Bras, R. L., Coe, M. T., Costa, M. H., Malhi, Y., Longo, M., Knox, R. G., McKnight, S., Wang, J., & Moorcroft, P. R. (2015). The fate of Amazonian ecosystems over the coming century arising from changes in climate, atmospheric CO_2, and land use. *Global Change Biology*, *21*(7), 2569–2587. https://doi.org/10.1111/gcb.12903

Zizka, A., Govender, N., & Higgins, S. I. (2014). How to tell a shrub from a tree: A life-history perspective from a South African savanna. *Austral Ecology*, *39*, 767–778.

SUPPORTING INFORMATION

Additional supporting information may be found in the online version of the article at the publisher's website.

How to cite this article: Smith, R. J., Singarayer, J. S., & Mayle, F. E. (2022). Response of Amazonian forests to mid-Holocene drought: A model-data comparison. *Global Change Biology*, 28, 201–226. https://doi.org/10.1111/gcb.15929